American Mineralogist, Volume 71, pages 17–37, 1986

The mineralogy of K-richterite-bearing lamproites

CHRISTIANE WAGNER AND DANIELLE VELDE

Laboratoire de Pétrologie Minéralogique
(U.A. 0736 du CNRS)
Université Pierre et Marie Curie (Paris 6)
4, Place Jussieu, 75230 Paris Cedex 5, France

Abstract

The mineralogy and chemistry of eleven phlogopite-richterite-bearing lamproites has been studied. It has been found that this mineral assemblage (also found in metasomatically altered ultrabasic xenoliths) is typical of peralkaline lamproites. These lavas are typically potassium- and magnesium-rich, with a positive correlation between these two elements, and consequently between peralkalinity and magnesium content. Titanium contents are variable, but may reach 7% TiO_2. The peralkaline character was acquired before crystallization, all minerals, including the first magmatic phases, having extremely low Al contents. Loss of alkalis, after partial or complete solidification, can be demonstrated in some specimens. Typical associations include besides phlogopite and richterite, Cr-rich Al-poor spinels, olivine, diopside, Ti-rich oxides (ilmenite, pseudobrookite, priderite). The peralkaline character is emphasized by the presence of roedderite-like phases in two specimens.

An electron microprobe study of lamproite minerals shows a general tetrahedral deficiency in most Al-bearing silicates, the sum Si + Al being systematically lower than its theoretical value. Most elements are regularly partitioned between co-crystallizing phases: e.g., Fe, Mg and Ti between richterite and phlogopite; Na and K between feldspar and richterite; tetrahedral deficiency between phlogopite and richterite.

These observations lead to the conclusion that the peralkaline character of these lamproites imposes constraints on the mineral compositions. However, the mineral compositions are not affected by the whole-rock silica saturation.

Xenocrystic material has been identified and is abundant in lamproites. Isolated relic crystals correspond to most major phases, except for richterite, that crystallize from the liquid, i.e., olivine, clinopyroxene, mica, ilmenite, pseudobrookite and apatite.

A comparison can be made between major authigenic phases from lamproites and equivalent phases from associations interpreted, in ultrabasic nodules, as metasomatic assemblages and presumed to have formed in the mantle under high pressures. Most major element partitioning trends are not affected by pressure but Ti solubility in silicates is considerably reduced by increasing pressure.

The origin of lamproitic liquids cannot be linked to basaltic magmas; basalts are indeed absent from lamproitic provinces. The observed bulk composition of lamproites could result from melting of richterite + phlogopite-bearing ultrabasic associations in the mantle. Calculations indicate that for all specimens considered in the present study the initial proportions could be richterite 30–50% and phlogopite 56–68%. Precipitation of olivine (with or without diopside) could then lead to the observed lamproitic lava compositions.

Introduction

The term lamproite was coined by Niggli (1923, p. 105) for rocks whose compositions were extreme with respect to their potassium and magnesium (high) and aluminum (low) contents. The term has been used since, to designate rocks with compositions similar to those of lamprophyres, but whose field relations clearly indicate a volcanic situation (Velde, 1969, 1975).

Recent definitions take into account mineralogical compositions. The term is thus restricted by Rock (1984) to volcanic or subvolcanic rocks with a unique paragenesis that includes the rare minerals, K-richterite and priderite. According to Scott Smith and Skinner (1984), current research shows that "lamproites are characterized by Ti-rich silicates and oxides, while the absence of plagioclase and significant amounts of melilite separates them from other potassium-rich alkaline rocks." Lamproite is used in the present work in Rock's general definition but, as pointed out by Scott Smith and Skinner (1984), the presence of Ti-rich silicates and oxides definitely appears to characterize this group of lavas.

0003–004X/86/0102–0017$02.00

Table 1. List of the samples studied, geographical localization, age, mineral assemblages and references to previous studies

	Localities	Specimen number	Rock type	Age	Mineralogical Assemblage	References
	SPAIN				Ol+Cpx+Phl+Richt+Kspar+Cr+Ilm	Lewis (1882) Osann (1906) Jeremine and Fallot (1929)
1	Cancarix, Albacete	74A1	Cancalite	5.7 to 7.6 m.y.	Ac+Ap+"Roed"+Ru+Cc X-Ol ? X-Cr ?	Hernandez Pacheco (1935) San Miguel de la Camara et al. (1952)
2	Calasparra. Murcia	72A7		Bellon et al.(1981) Bellon (1976;1981)	Ap+Glass+X-Ol ?	Fuster and Gastesi (1965) Fuster et al.,(1967).
3	Jumilla, Murcia	11A8	Jumillite	Nobel et al. (1981)	Lc+Ac+Ap+Glass	Borley (1967) Velde (1969)
4	Barqueros, Murcia	73A8	Fortunite	Montenat et al. (1975)	Psb+Glass X+Phl+X-Al-Sp+X-Psb+X-Ilm+X-Ru	Ruiz and Badiola (1980) Nixon et al. (1982)
	UNITED STATES					
5	Smoky Butte, Montana	7B8	Lamproite	27 m.y. Marvin et al.(1980)	Ol(alt.)+Cpx+Phl+Richt +Kspar+Anal+Ap+Glass +Psb+Prid+Cr	Matson (1960) Velde (1975)
6	Shiprock dyke, New Mexico	5B6	Minette	27-30 m.y. Naeser (1971) Armstrong (1969)	Ol(alt)+Cpx+Phl+Richt- Arfv+Kspar+Ap+Glass+ Ilm+Mt+Ac	Williams (1936) Nicholls (1969) Velde (1969) Roden (1981)
7	Moon Canyon, Utah	MC77	Lamproite	36-40 m.y.	Ol(alt)+Cpx+Phl+Richt+ Kspar+Ap+Glass+Ilm+ Psb+"Roed"+Cr+X-Phl	Crittenden and Kistler (1966) Best et al. (1968)
	FRANCE					
8	Sisco, Corsica	61A3	Minette	15.4-13.5. m.y. Feraud et al.(1977) Civetta et al.(1978) Bellon (1981)	Ol(alt)+Cpx+Phl+Richt- Arfv+Kspar+Ilm+Prid+Cr +Ru+Ap+Sph+Cc	Velde (1967)
9	Sisco, Corsica	8A12				Velde (1968)
	AUSTRALIA					Wade and Prider (1939)
10	Mount North, West Kimberley	SO136	Wolgidite	17-22 m.y. Jaques et al. (1982)	Ol(alt)+Cpx+Phl+Richt+ Lc+Ilm+Prid+Ap+Glass	Carmichael (1967) Kaplan et al. (1967) Mitchell (1981) Jaques et al. (1984)
	ITALY					
11	Orciatico, Pisa	60A7	Selagite	4-1 m.y. Borsi et al. (1967)	Ol+Cpx+Phl+Kspar+Ilm +Richt+Cr+Ap	Barberi and Innocenti (1967) Stefanini (1934)

Abbreviations : Ac, acmite ; Al-Sp, aluminous spinel ; Anal, analcite ; Arfv, arfvedsonite ; Cc, calcite ; Cpx, clinopyroxene (diopside) ; Cr, chromite ; Ilm, ilmenite ; Kspar, potassium feldspar ; Lc, leucite ; Mt, magnetite ; Ol, olivine ; Ol(alt), altered olivine ; Phl, phlogopite ; Psb, pseudobrookite ; Prid, priderite ; Richt,richterite ; "Roed", roedderite-like phase ; Ru, rutile ; Sph, sphene. X indicates that the species whose abbreviated name follows is present, but interpreted as a xenocryst.

The phlogopite–K-richterite association is also recorded from nodules found in kimberlites, the MARID suite as defined by Dawson and Smith (1977). The mineralogical associations as well as the composition of the phases present is similar in the nodules and in the lamproites. It seemed warranted to examine the compositions of these phases and their crystallization relationships in lamproites and consider more closely the similarities and differences between the constituent minerals of lamproites and the metasomatic assemblages from mantle rocks that could be the source of lamproites.

Experimental bulk rock analyses were performed using a Philips PW 1400 spectrometer. Ferrous iron was determined using a method outlined by Peck (1964) and H_2O^+ by a modified Penfield method.

Electron microprobe analyses were carried out on an MS-46 CAMECA instrument with natural or synthetic minerals as standards for olivines, micas, amphiboles and clinopyroxenes. Counting time = 30 s; accelerating voltage = 15 kV; current = 30 nA (20 nA for K and Na in micas and amphiboles). Other mineral compositions were determined with a CAMEBAX automated electron microprobe using either oxides or natural minerals as standards. Counting time = 30 s; accelerating voltage = 15 kV; current = 30 nA for oxides; 5 nA for feldspars.

Chemical composition and peralkaline character of the lamproites

The eleven specimens studied in this paper come from most of the classical localities. Their ages vary from 40 to 4.1 m.y.; they usually occur as pipes, dikes or necks but flows are also found. Table 1 gives the list of all samples studied and Table 2 the corresponding bulk chemical compositions.

Lamproites are magnesium-rich: their CIPW norms show 20% normative enstatite (or diopside) with or without forsterite. They are potassium-rich, and analyses show a positive correlation between potassium and magnesium, a significant difference with usual trends in magmatic series. No correlation is observed between alkalis and iron content. In the specimens studied, K_2O varies between 7 and 12% (except the Jumilla specimen where the present K_2O content is only 3.7%), and is largely superior to Na_2O. Titanium contents are variable, and can reach 7% TiO_2. This is particularly striking when considered in connec-

Table 2. Chemical composition of the samples studied. All analyses are new but for Nos. 6, 8, 10

	1	2	3	4	5	6	7	8	9	10	11
	74A1	72A7	11A8	73A8	7B8	MC72	5B6	SO136	61A3	8A12	60A7
SiO_2	55.41	56.61	47.31	58.77	51.41	55.73	53.70	45.82	57.46	56.23	57.81
Al_2O_3	8.83	7.96	6.52	11.34	8.36	10.72	11.06	6.86	10.88	12.06	10.94
Fe_2O_3	1.17	2.12	3.83	1.31	3.02	3.73	3.57	6.07	1.46	1.91	3.55
FeO	3.40	3.13	2.88	3.49	2.31	0.95	3.08	1.98	2.54	2.91	1.44
MgO	13.59	12.45	17.16	9.22	8.05	6.96	7.86	10.90	7.24	6.90	8.26
CaO	3.97	2.97	8.82	2.71	4.71	3.85	7.38	4.70	2.96	3.48	4.43
Na_2O	1.13	0.75	1.88	1.08	1.25	1.21	2.31	0.84	1.14	1.03	1.09
K_2O	8.63	9.21	3.71	8.46	7.87	10.49	6.64	8.82	10.75	10.00	7.94
MnO	0.08	0.08	0.12	0.10	0.06	0.08	0.10	0.10	0.05	0.07	0.07
TiO_2	1.41	1.61	1.32	1.35	5.46	2.82	1.81	7.34	2.19	1.14	1.37
P_2O_5	1.35	1.23	2.00	0.79	2.22	1.13	0.91	1.83	0.74	0.79	0.72
BaO						0.35		1.27			
CO_2								0.08		0.41	
H_2O+	0.59	1.86	3.77	0.96	3.58	1.14	1.53	0.75	1.70	1.56	1.18
H_2O-	0.23	0.65	1.31	0.31	1.74	0.89	0.62	2.40	0.72	1.58	1.06
F	0.36	0.41	0.32	0.30	0.46		0.16		0.38	0.35	0.33
Clppm	226	321	174	87	78				45	319	74
Total	100.15	101.04	100.95	100.19	100.50	100.05	100.73	99.76	100.21	100.42	100.19
$O \equiv F$	0.15	0.17	0.13	0.13	0.19		0.07		0.16	0.15	0.14
Total	100.00	100.87	100.82	100.06	100.31		100.66		100.05	100.27	100.05
$\frac{Na+K}{Al}$	1.27	1.41	1.09	0.96	1.26	1.24	0.99	1.59	1.24	1.04	0.95
Q		2.90		2.27	3.14				2.33		4.61
Or	48.15	43.37	21.90	50.04	45.65	58.53	39.25	37.25	59.32	59.10	46.98
Ab			12.42	9.12			17.34			6.36	9.22
An				1.06			0.14				1.45
Ac	3.37	5.57	2.68		8.73	9.02		6.47	4.20	2.08	
Ne			0.23				1.19				
Ns	1.33				0.16				1.13		
Ks	0.80	3.08			0.26	0.96		4.16	1.18		
Di	8.65	5.29	24.07	5.75		4.34	23.80		7.76	7.92	12.33
En	21.20	28.87		20.77	20.13	15.32		27.20	14.69	10.55	14.94
Fs	2.44	2.85		3.92					0.92	1.60	
Fo	6.30		22.35				6.03			2.38	
Fa	0.80		0.53							0.40	
Mt		0.28	4.20				5.01			1.73	0.90
Hem						0.61	0.11	4.00			2.93
Ilm	2.68	3.05	2.51	2.57	5.00	2.18	3.44	4.41	4.16	2.17	2.60
Tn					6.39	3.85		1.37			
Pf						0.18		6.12			
Ru					0.22			0.88			
Ap	3.19	2.92	4.70	1.88	5.24	2.73	2.15	4.03	1.75	1.73	1.71
Cc								0.20		0.93	

Analysis 6, Best et al., 1968; Analysis 8, Wade and Prider, 1940; Analysis 10, Velde, 1967.

tion with the low iron content of these rocks in general (4.0 to 6.7% FeO + Fe_2O_3 and 8% in specimen SO136).

The specimens examined are either definitely peralkaline or close to peralkalinity. This character is demonstrated by the presence of normative acmite in the CIPW norm, accompanied by sodium and/or potassium metasilicate, the maximum content of normative anorthite being 1.45% (Table 2). Fluorine (between 0.2 and 0.47%) is positively correlated with potassium content following the relationship discovered by Aoki et al. (1981).

Two lines of evidence indicate the primary origin of the peralkaline character of the lamproitic magma. One argument is the fact that lamproites often occur with glassy textures, frequent among the Spanish lamproites, present in Smoky Butte and the Leucite Hills, and recently described in Australia (Prider, 1982). The second line of evidence is that the spinels found in olivines of the Spanish lamproites, Sisco, Moon Canyon, the selagites and the Smoky Butte lamproite are uncommonly chrome-rich (51 to 65% Cr_2O_3) but always alumina-poor (0.23% to 4% Al_2O_3) (Table 3). In comparing data on various olivine-bearing lavas, it appears that the Al_2O_3 content of Cr-rich spinels is related to the composition of the rocks in which they are found. Using, for example, analyses published by

Table 3. Representative electron microprobe analyses of chrome spinels found as inclusions in the olivines. Fe^{3+} calculated assuming 3 cations and 4 oxygens

	1	2	3	4	5	6	7	8	9	10	11
	74A1	74A1	72A7	72A7	11A8	11A8	73A8	6B18	8A12	60A7	60A7
Al_2O_3	0.23	0.15	3.04	1.72	2.00	1.16	1.10	0.71	4.16	3.56	1.87
Cr_2O_3	51.41	62.64	65.34	61.43	55.78	51.48	31.58	42.78	63.00	55.64	36.22
FeO	37.05	26.40	20.33	29.99	29.34	34.97	46.72	32.84	15.31	30.17	47.95
MgO	4.42	8.00	10.41	4.72	9.80	7.43	5.24	9.54	13.80	5.77	3.30
MnO	0.84	0.82	0.69	0.90	0.79	0.47	0.55	0.61	0.48	0.80	0.86
TiO_2	4.52	1.16	1.23	1.63	1.03	0.79	10.90	9.50	2.14	1.12	5.70
ZnO	nd	nd	nd	nd	nd	nd	nd	0.32	0.20	nd	nd
Total	98.47	99.17	101.04	100.39	98.74	96.30	96.09	96.30	99.09	97.06	95.90
Fe_2O_3	9.77	7.18	3.22	4.54	13.32	16.39	15.79	9.59	2.97	7.73	19.27
FeO	28.26	19.94	17.43	25.90	17.35	20.23	32.51	24.22	12.64	23.21	30.61
Al	0.010	0.006	0.120	0.072	0.081	0.049	0.048	0.030	0.163	0.151	0.082
Fe3+	0.267	0.190	0.081	0.121	0.345	0.444	0.436	0.257	0.074	0.209	0.538
Cr	1.476	1.742	1.736	1.720	1.520	1.464	0.916	1.205	1.656	1.580	1.062
Fe2+	0.858	0.587	0.490	0.767	0.500	0.609	0.997	0.721	0.351	0.697	0.949
Mg	0.239	0.420	0.522	0.249	0.504	0.399	0.286	0.506	0.684	0.309	0.182
Mn	0.026	0.024	0.020	0.027	0.023	0.014	0.017	0.018	0.014	0.024	0.027
Ti	0.123	0.031	0.031	0.043	0.027	0.021	0.301	0.254	0.053	0.030	0.159
Zn								0.008	0.005		

FeO° = Total iron as FeO
nd : not sought for.

Eissen (1982) on MORB basalts and Barbot (1983) on spinels from alkali basalts, it can be seen that for a given Cr content, spinels from tholeitic basalts are richer in Al_2O_3 than spinels found in alkali basalts. Within the field of alkaline rocks, spinels are richer in aluminum in alumina saturated melilite-bearing compositions than they are in peralkaline compositions, the two fields showing no overlap (Velde and Yoder, 1983; unpublished data). In the lamproites the Cr-rich spinels can be considered as the liquidus phase. From their rather unique composition, they definitely belong to the peralkaline field as defined by Velde and Yoder (pers. com.). The peralkaline character of the lamproites could, in some instances, have been more pronounced than presently evidenced by their bulk composition. Specimen 11A8, from Jumilla, contains apatite phenocrysts with frequent glass inclusions. One of these (0.06 × 0.03 mm) contains besides glass, a euhedral crystal of olivine and a small mica blade, both phases appearing as phenocrysts in the rock. This glass (Table 4) is considerably richer in alkalis than the bulk rock and the (Na + K)/Al of the glass inclusion is 1.72 as opposed to 1.09 for the bulk rock composition. Least squares calculations made to estimate whether the glass composition could be derived from the bulk composition of the rock, taking into account the presence of the olivine and biotite crystals, show that a reasonable fit is obtained only if it is assumed that the bulk composition has lost alkalis (mostly potassium) after inclusion of the glass in the apatite.

Table 4. Electron microprobe analyses of the glass (1 = average of 3 determinations) and olivine (2) included in an apatite crystal from specimen 11A8

	1	2
SiO_2	55.00	40.00
Al_2O_3	12.00	
FeO°	6.00	11.00
MgO	1.30	50.00
CaO	1.60	0.20
Na_2O	5.00	
K_2O	12.00	
MnO		0.20
TiO_2	2.60	
Total	95.50	101.40

FeO° = Total iron as FeO

From the above one can consider that the lamproite liquids that produced phogopite and K-richterite assemblages had primary peralkaline compositions. This character was acquired before the first liquidus phase (Cr-spinel) crystallized. In at least one specimen (11A8) it can be demonstrated that the composition was altered after the crystallization of the feldspar (see below) and originally had a stronger peralkaline characteristic.

Finally, the silica saturation is not a factor critical to the mineralogical association under consideration since lamproite compositions can vary from undersaturated with respect to silica (with modal felspathoid) to oversaturated (with modal quartz).

Table 8. Representative electron microprobe analyses of feldspars from the lamproites studied. Total iron = Fe_2O_3

	1	2	3	4	5	6	7	8	9	10	11	12	13
	74A1	72A7	11A8	11A8	73A8	7B8	5B6	5B6	MG77	61A3	61A3	60A7	60A7
SiO_2	63.90	63.91	61.28	63.11	63.81	63.61	63.22	65.02	63.23	64.24	64.63	64.99	64.65
Al_2O_3	17.46	17.12	12.85	14.49	18.59	15.76	19.00	18.41	15.86	17.29	18.24	18.57	18.52
Fe_2O_3	1.12	1.26	4.95	3.17	0.31	1.93	0.62	0.62	2.91	1.14	0.20	0.51	0.78
MgO	0.02	0.03	0.10	0.20					0.08				
CaO							0.11	0.10					
Na_2O	0.44	0.63	0.66	0.32	1.39	0.55	3.25	3.53	0.32	0.42	0.56	2.25	2.29
K_2O	16.15	15.75	16.38	16.20	14.50	15.83	10.98	11.52	15.84	16.21	15.97	13.34	12.98
BaO	0.25	0.39	0.11	0.08	0.64	1.21	1.87		0.50	0.11	0.34	0.06	0.89
TiO_2	0.27	0.29	0.42	0.22	0.16	0.33		0.26	0.29	0.12	0.07	0.17	0.40
Total	99.61	99.38	96.75	97.79	99.40	99.22	99.05	99.46	99.03	99.53	100.01	99.89	100.51
Si	2.986	2.993	3.012	3.028	2.969	3.013	2.945	2.980	2.994	3.000	2.994	2.982	2.966
Al	0.962	0.945	0.745	0.820	1.020	0.880	1.043	0.995	0.885	0.952	0.996	1.004	1.002
Fe3+	0.039	0.044	0.183	0.114	0.011	0.069	0.022	0.021	0.104	0.040	0.007	0.018	0.027
Mg	0.001	0.002	0.007	0.014					0.006				
Ca							0.005	0.005					
Na	0.040	0.057	0.063	0.030	0.125	0.051	0.294	0.314	0.029	0.038	0.050	0.200	0.204
K	0.963	0.941	1.027	0.992	0.861	0.957	0.653	0.674	0.957	0.966	0.944	0.781	0.760
Ba	0.005	0.007	0.002	0.002	0.012	0.023	0.034		0.009	0.002	0.006	0.004	0.016
Ti	0.009	0.010	0.016	0.008	0.006	0.012		0.009	0.010	0.004	0.002	0.006	0.014
	5.005	5.001	5.050	5.008	5.003	5.004	4.996	4.997	4.994	5.002	4.999	4.992	4.988

Mineralogy

A general order of crystallization can be deduced from the textural relationships of the lamproites studied. In all specimens olivine appears to be the first silicate phase to appear. The Cr-rich spinels are only found as inclusions in olivine. Diopside and phlogopite have probably syncrystallized; amphibole and feldspar have appeared subsequently and are contemporaneous with an acmitic rim on the clinopyroxenes and in some instances with a deeply red colored edge around the phlogopites. Oxides appear to have formed after the diopside and the phlogopitic centers of the micas. The specimen from Moon Canyon shows phlogopite surrounding olivine crystals, and richterite rimming the diopside, thus supporting the order stated. It should also be mentioned that, when present, feldspar often shows a skeletal habit. Modal analyses are given in Table 5.[1]

Olivine

Olivine is found unaltered only in some Spanish specimens and the Orciatico selagite. In both types, some crystals (usually anhedral, and large in size) represent xenocrysts with typical kink-bands. Phenocrysts are generally euhedral in outline, and contain numerous euhedral spinel inclusions. Compositions of the xenocrysts are similar to that of the cores of the phenocrysts, in major elements (Fo%) or trace elements (Ni for example). Compositions, including xenocrysts (Table 6[1]) vary from 92 to 77% Fo. Nickel contents are consistently high, vary from 0.10 to 0.70% NiO, but usually occur between 0.30 and 0.50%. Such high Ni contents are above the values given for olivine in basalts (between 0.10 and 0.30 NiO, Simkin and Smith, 1970; Anderson and Wright, 1972). They are comparable to values reported by Reid et al. (1975) in olivine from peridotite xenoliths, close to Ni contents found in olivines from nodules occurring in kimberlites (Nixon and Boyd, 1973; Scott, 1981) and similar also to values recently determined in the Australian lamproites and kimberlites (Jaques et al., 1984).

The NiO content of the olivines is inversely correlated with the fayalite content. In the selagite, the most ferrous olivine (Fo_{77}) contains 0.23% NiO. Calcium in the olivines is usually low, particularly in the xenocrysts, but always below 0.20% CaO. There is a positive correlation between CaO and fayalite contents of the olivine.

The manganese contents are consistently high and positively correlated with the fayalite content; MnO is close to 0.30% at Fo_{80}.

Pyroxene

Clinopyroxene (Table 7[1]) in the lamproites studied falls mostly in the endiopside field of the pyroxene quadrilateral. Its abundance varies from 6 to 22% in volume. It most often occurs as unzoned phenocrysts which contain around 1% TiO_2. The Cr_2O_3 content varies between 0.1 and 0.3 but, in the Spanish lamproites falls in the 0.4–0.9% range. These values are considerably higher than those commonly found in lavas and are, for the highest ones, consistent with percentages recorded from diopsides from dunite inclusions (e.g., Berger, 1981).

In all samples, save the specimen from Shiprock (5B6), the tetrahedral site of the pyroxene is incompletely filled by Si and Al; the tetrahedral site occupancy varies from 1.94 to 2.00, usually being between 1.97 and 1.98 atoms. The site can be considered as completed by Fe^{3+} atoms that are present when the structural formula is calculated on 4 cations and 6 oxygens. This deficiency in Si + Al was noted by Carmichael (1967) for the Leucite Hills diopside and is mentioned by Jaques et al. (1984) for the Australian lamproites. This situation can be related to the low-alumina content of the liquid from which the pyroxenes crystallized. Acmite is present in many samples, as a thin, late rim around the diopside crystals, or small groundmass grains.

[1] To receive copies of Tables 5, 6, 7, 14, 15, and 16, order Document AM-86-292 from the Business Office, Mineralogical Society of America, 1625 I Street, N.W., Suite 414, Washington, D.C. 20006. Please remit $5.00 in advance for the microfiche.

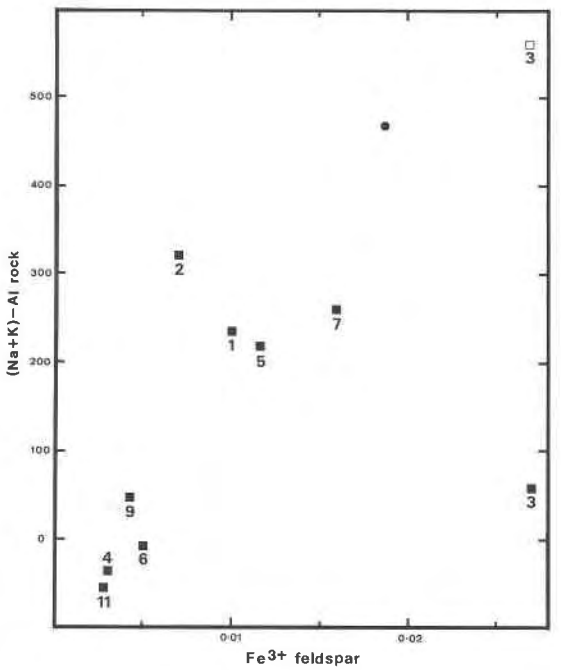

Fig. 1. The joint distribution of (Na + K) − Al calculated from the bulk rock composition and the Fe^{3+} content of feldspar (mole%). Solid squares: data from this study (specimen numbers are listed in Table 1); solid circle: LH9, Carmichael (1967). Open square: Jumilla composition corrected for calculated alkali loss.

In two specimens (Shiprock, 5B6 and Smoky Butte, 7B8) some of the colorless diopside phenocrysts show a green center. In Shiprock the green cores are richer in Al, Fe and Na than the diopside zone. Barton and Bergen (1981) have reported the presence of green clinopyroxenes with a salitic composition in a Leucite Hills wyomingite, and this type of clinopyroxene has frequently been found in alkali-rich, potassic rocks (Barton and Bergen, 1981; Lloyd, 1981). These green centers in diopsides are commonly interpreted as being xenocrysts, coming from the disaggregation of clinopyroxenite nodules, and appear to be a ubiquitous feature of potassic volcanics.

Feldspar

Feldspar is abundant (19 to 48% in volume) and appears late in the crystallization sequence; it is absent from the Mount North Australian lamproite which carries leucite and from some of the glassy specimens. In all but two cases the feldspar composition is close to that of the potassic end member (Or 95–98). Feldspars from the Shiprock and Barqueros specimens are more sodic (64 to 72, and 87 to 89% Or respectively) (Table 8).

Iron contents are high, usually varying between 1 and 2% Fe_2O_3, but reaching 2.5% at Moon Canyon and 5% in the jumillite. Carmichael (1967) reports values between 3 and 4% in the Leucite Hills lamproites and Best et al. (1968) 3.83% in some of the Moon Canyon specimens. According to Smith (1974) the iron content of feldspars could be related to a rapid growth rate. Though feldspars in lamproites have crystallized rapidly as exemplified by their common skeletal habit, the iron content cannot be exclusively linked to the growth rate, but can definitely be correlated with the peralkalinity of the liquid (Fig. 1). The only exception is the Jumilla feldspar whose abnormal position on the diagram is consistent with the alkali loss already addressed above.

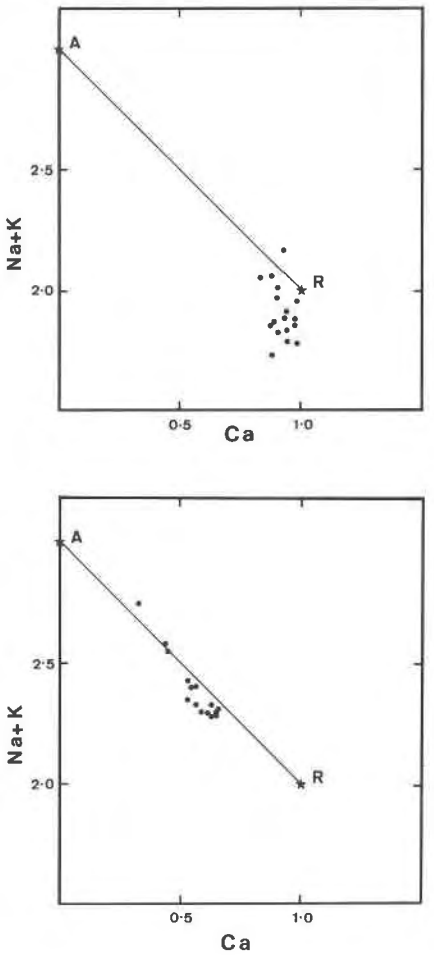

Fig. 2. (a) The distribution of Na + K and Ca in richterites from specimen 7B8. (b) The distribution of Na + K and Ca in richterites from specimen 5B6.

The feldspars are titanium-rich. Percentages of TiO_2 in the lamproite feldspars analyzed reach 0.45%; Best et al. (1968) give 0.50% for a Moon Canyon feldspar, values that are considerably higher than the 0.07 to 0.08% recorded by Smith (1974) in his treatise. Feldspars from the Sisco minette, which coexist in the groundmass with abundant minute sphene needles, show the lowest values (0.07% TiO_2). No simple relationship is apparent between the TiO_2 content of the feldspars and the TiO_2 content of the liquid from which they crystallized.

Barium varies betwen 0.1 and 0.3% BaO, but can reach 0.62% (73A8) and 1.3% (7B8). Two specimens show large variations in the barium contents of the feldspar: in sample 60A7, BaO varies from 0 to 0.89%, and in sample 5B6 from 0.0 to 3.22% BaO. In both cases there is an inverse correlation between BaO and the sum $Na_2O + K_2O$.

Amphibole

Amphiboles found in peralkaline lamproites belong to the richterite group and are characterized by the presence of a high proportion of potassium in the A site. They are among the last phases to appear and are found, albeit in small amounts, even in some lamproites that do not have a peralkaline composition (e.g., the selagite). In this case, their presence indicates that towards the

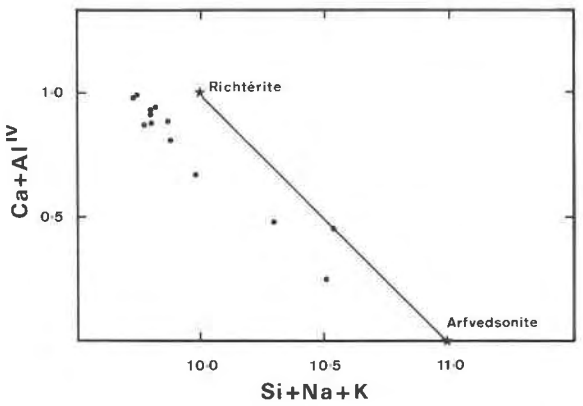

Fig. 3. The distribution of Ca + Al^{IV} and Si + Na + K in richterites from specimen 61A3.

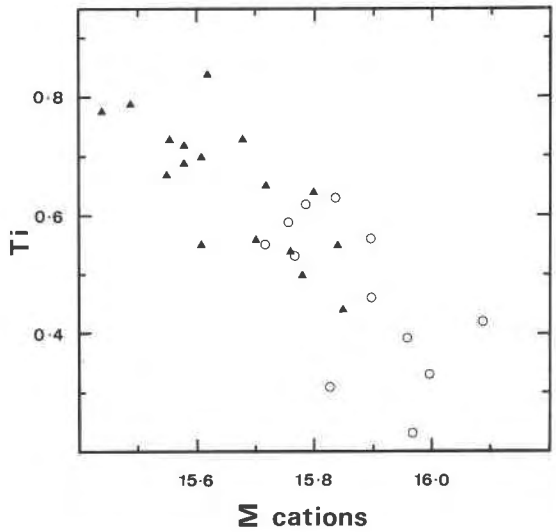

Fig. 4. The distribution of Ti and the sum of cations in richterites from 74A1 (solid triangles) and 72A7 (open circles).

end of the crystallization sequence at least the residual liquids were peralkaline. Richterites belong to the calcalkaline amphibole group and their general formula can be written $(Na,K)NaCa(Mg,Fe^{2+})_5Si_8O_{22}(OH)_2$. The richterites analyzed have at most one Fe^{2+} atom in the C site, except for the amphiboles found in the Shiprock and Sisco specimens that are richer in iron (varying between Mg_2Fe_3 and Mg_3Fe_2).

Their composition is usually close to the theoretical richterite composition (e.g., 7B8, Fig. 2a), or intermediate (as in Shiprock, Fig. 2b) between richterite and arfvedsonite (Table 9). The structural formulae were computed following the method of Papike et al. (1974) as advocated by Leake (1978). Initially the A site (Na + K) is overfilled and the tetrahedral site is underfilled (Si + Al < 8). In Figure 3 the trend shown by the experimental points is parallel to the theoretical richterite-arfvedsonite line demonstrating this tetrahedral deficiency. The tetrahedral site must then contain another ion which could be Fe^{3+}. When calculated Fe^{3+} is assigned to the tetrahedral site, the structural formula usually becomes acceptable, the tetrahedral site is filled and there is no excess of ions in the A site. In some analyses however (e.g., in Calasparra) the tetrahedral site cannot be filled by Si, Al and Fe^{3+} and the presence of yet another ion should be considered.

The richterites are Ti-rich: the minimal values found are close to 2% TiO_2, in Sisco for example, but reach 9% in Moon Canyon. In amphiboles with high Ti contents (Cancarix, Calasparra and

Table 9. Representative electron microprobe analyses of K-richterites from the lamproites studied. Structural formulae calculated on the basis of 23 oxygens

	1	2	3	4	5	6	7	8	9	10	11	12	13	14	15	16
	74A1	74A1	72A7	11A8	11A8	73A8	7B8	5B6	5B6	MC77	MC77	61A3	8A12	SO136	SO136	60A7
SiO_2	52.89	52.92	51.79	52.31	53.22	54.40	53.26	51.10	48.85	51.12	50.06	51.55	52.02	52.46	51.24	54.50
Al_2O_3	0.41	0.55	0.36	1.01	0.32	0.33	0.38	1.75	1.62	0.51	0.25	0.36	0.40	0.33	0.53	0.93
FeO°	4.51	13.64	6.62	7.99	9.55	7.08	4.22	13.21	17.85	5.53	8.29	16.78	12.35	2.94	5.45	8.05
MgO	18.65	11.17	17.24	17.09	16.70	18.58	18.93	15.02	12.36	17.06	14.68	10.14	16.25	20.55	18.12	18.13
CaO	6.68	4.44	5.79	3.51	4.05	5.84	6.37	3.87	1.99	6.38	4.30	1.21	6.44	6.58	6.68	8.34
Na_2O	4.24	4.67	4.75	6.33	6.43	5.01	4.27	6.95	8.26	4.33	4.96	6.66	3.85	3.29	3.64	3.40
K_2O	3.64	4.12	3.69	2.89	2.94	2.51	4.25	1.62	1.52	4.22	3.94	4.34	3.56	5.87	5.55	1.32
MnO			0.10	0.13	0.14	0.09	0.22	0.17	0.21	0.12	0.11	0.04	0.24	0.04	0.05	0.11
TiO_2	5.14	7.16	5.66	5.42	4.19	3.81	5.10	3.55	3.23	7.44	8.47	6.54	2.56	5.04	6.34	1.64
Total	96.16	98.67	96.00	96.68	97.54	97.65	97.00	97.25	95.88	96.71	95.06	97.62	97.67	97.10	97.60	96.42
Si	7.632	7.725	7.577	7.588	7.711	7.747	7.633	7.527	7.488	7.432	7.470	7.736	7.657	7.532	7.422	7.833
Al	0.069	0.094	0.062	0.173	0.055	0.055	0.065	0.303	0.293	0.087	0.044	0.063	0.069	0.055	0.090	0.157
Fe2+	0.544	1.665	0.809	0.969	1.157	0.843	0.506	1.627	2.288	0.672	1.035	2.106	1.520	0.353	0.661	0.967
Mg	4.011	2.430	3.759	3.695	3.606	3.943	4.043	3.299	2.824	3.697	3.265	2.267	3.565	4.397	3.911	3.884
Ca	1.033	0.694	0.908	0.546	0.629	0.891	0.979	0.611	0.326	0.994	0.688	0.194	1.016	1.012	1.037	1.285
Na	1.185	1.321	1.347	1.780	1.806	1.383	1.187	1.986	2.456	1.221	1.435	1.938	1.099	0.916	1.024	0.948
K	0.669	0.767	0.688	0.535	0.543	0.456	0.777	0.305	0.297	0.783	0.750	0.830	0.669	1.076	1.026	0.242
Mn			0.012	0.016	0.017	0.011	0.027	0.021	0.027	0.015	0.014	0.005	0.030	0.005	0.006	0.013
Ti	0.558	0.786	0.622	0.591	0.457	0.408	0.550	0.394	0.372	0.813	0.951	0.738	0.283	0.544	0.690	0.177
Total	15.701	15.485	15.784	15.892	15.980	15.737	15.767	16.073	16.370	15.726	15.652	15.877	15.908	15.890	15.867	15.506

FeO° = Total iron as FeO

Table 10. Representative electron microprobe analyses of micas from the lamproites studied. Structural formulae calculated on the basis of 11 oxygens

	1	2	3	4	5	6	7	8	9	10	11	12	13	14	15	16	17	18	19	20
	74A1	74A1	72A7	72A7	11A8	73A8	73A8	7B8	7B8	7B8	5B6	5B6	5B6	5B6	MC77	8A12	8A12	SO136	SO136	60A7
SiO_2	41.50	41.42	39.94	40.12	38.68	41.21	42.90	39.74	38.20	38.80	38.60	36.51	38.32	36.73	40.43	40.24	40.99	39.99	39.82	39.42
Al_2O_3	11.00	10.24	12.41	10.28	8.79	12.65	11.92	11.27	10.59	10.43	13.13	10.34	13.57	10.83	12.15	11.77	10.59	10.89	6.93	11.05
FeO°	5.11	7.63	3.07	6.53	11.49	6.92	3.87	3.88	6.95	7.71	4.79	11.16	5.76	11.82	2.70	4.41	11.78	4.13	10.66	11.03
MgO	20.79	18.19	24.44	19.69	16.24	22.18	24.60	22.12	18.51	18.21	23.26	15.59	21.79	17.37	25.17	23.73	17.51	23.31	19.63	17.63
MnO	0.03	0.01	0.01	0.04	0.08	0.06	0.03	0.02	0.03	0.04		0.12	0.03	0.10		0.05	0.13	0.01	0.10	0.10
TiO_2	6.88	9.51	3.90	8.78	11.19	4.79	1.98	7.04	9.13	9.93	3.14	8.50	3.73	9.43	2.30	3.38	5.11	5.49	7.95	6.25
Cr_2O_3	0.24	0.09	1.33	0.09	0.03	0.07	0.76	0.76	0.15	0.03	1.32		0.51		1.07	1.57	0.06	1.19	0.02	0.04
Na_2O	0.07	0.14	0.01	0.20	0.46	0.34	0.45	0.10	0.16	0.18	0.60	0.70	0.46	0.50	0.11	0.15	0.36		0.23	0.55
K_2O	9.42	9.33	10.24	9.63	8.30	9.48	9.87	9.63	9.13	8.86	10.74	9.97	10.84	10.56	11.12	10.53	10.38	11.39	11.00	8.96
BaO	0.84	0.61	0.05	0.51	2.11	0.19	0.08	1.11	2.80	2.62	0.34	0.31	0.33	0.28	0.13	0.13	0.29	0.12	0.55	1.53
Total	95.89	97.15	95.40	95.87	97.37	97.89	96.48	95.67	95.65	96.81	95.86	93.21	95.34	97.64	95.18	95.97	97.21	96.53	96.87	96.56
Si	2.949	2.936	2.837	2.882	2.883	2.880	2.997	2.843	2.810	2.818	2.777	2.791	2.779	2.693	2.888	2.870	2.974	2.849	2.929	2.888
Al	0.921	0.855	1.039	0.871	0.759	1.042	0.982	0.950	0.918	0.893	1.113	0.932	1.160	0.938	1.020	0.990	0.906	0.915	0.601	0.953
Fe2+	0.303	0.452	0.182	0.392	0.704	0.405	0.227	0.233	0.428	0.469	0.285	0.713	0.350	0.725	0.162	0.263	0.715	0.246	0.656	0.676
Mg	2.203	1.922	2.588	2.108	1.773	2.310	2.562	2.359	2.030	1.971	2.495	1.776	2.355	1.898	2.681	2.523	1.893	2.476	2.152	1.925
Mn	0.002	0.001		0.003	0.005	0.004	0.002	0.001	0.002	0.003		0.008	0.002	0.008		0.003	0.008	0.001	0.006	0.006
Ti	0.368	0.507	0.209	0.474	0.616	0.252	0.104	0.379	0.505	0.543	0.170	0.489	0.204	0.520	0.124	0.182	0.279	0.294	0.440	0.339
Cr	0.014	0.005	0.075	0.005	0.001	0.004	0.042	0.043	0.009	0.002	0.076		0.029		0.060	0.089	0.004	0.067	0.007	0.002
Na	0.010	0.019	0.001	0.028	0.065	0.046	0.062	0.015	0.023	0.025	0.083	0.105	0.065	0.072	0.015	0.021	0.051		0.033	0.079
K	0.854	0.843	0.928	0.882	0.776	0.846	0.879	0.879	0.857	0.821	0.986	0.973	1.004	0.988	1.013	0.958	0.961	1.035	1.032	0.837
Ba	0.023	0.017	0.001	0.014	0.061	0.005	0.003	0.031	0.081	0.075	0.010	0.009	0.010	0.008	0.004	0.004	0.008	0.004	0.016	0.044
Total	7.647	7.557	7.860	7.659	7.593	7.794	7.860	7.733	7.663	7.620	7.995	7.796	7.958	7.850	7.967	7.903	7.799	7.888	7.866	7.751

FeO° = Total iron as FeO

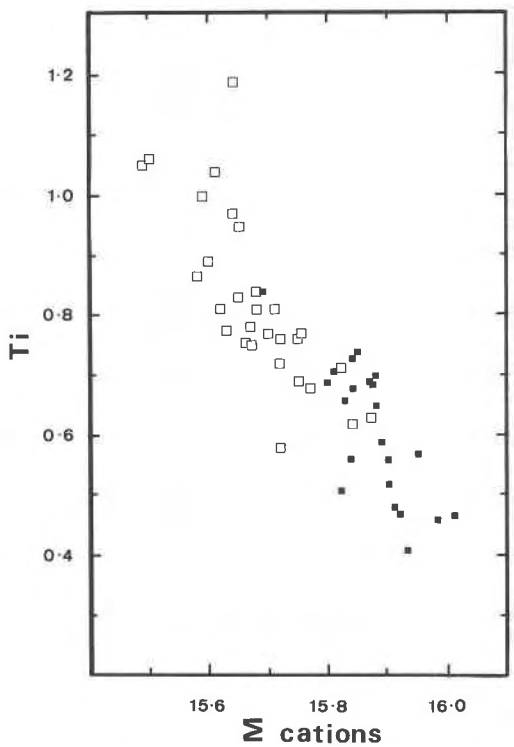

Fig. 5. The distribution of Ti and the sum of cations in richterites from MC77 (open squares) and 11A8 (solid squares).

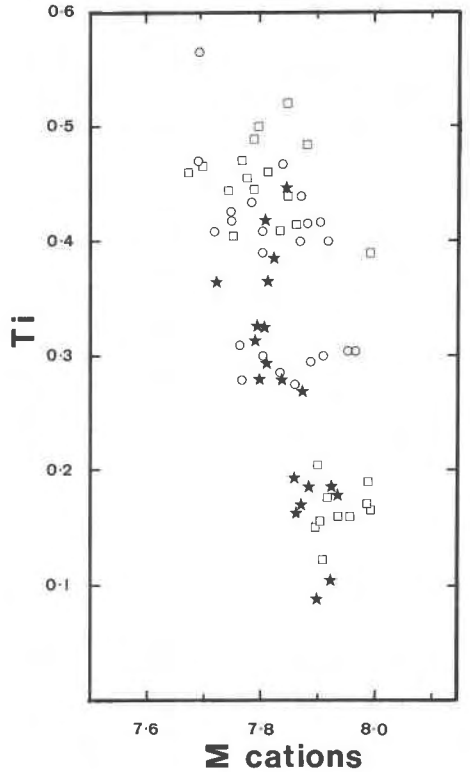

Fig. 6. The distribution of Ti and the sum of cations in phlogopites from 3 specimens. Open squares, 5B6; open circles, SO136; solid stars, 8A12.

Moon Canyon) the inclusion of titanium creates a vacancy in the structure as can be shown on a diagram showing the variation of Ti vs. the sum of ions (Figs. 4 and 5), an analogous situation to that described below in trioctahedral micas. Amphiboles with lower Ti-contents from all other specimens display a negative correlation between titanium content and the number of Si + Al ions on the tetrahedral site, but no relationship is found between Ti content and the sum of cations.

Some amphiboles are zoned: richterite from the Cancarix and Australian specimens show a darker color towards the rims of the crystals, and this variation corresponds to an increase in titanium and iron and a decrease in magnesium without any significant variation of the other elements, probably indicating the substitution $\square + Ti + Fe^{2+} = 3Mg$.

The main difference between these amphiboles and richterites found in the MARID suite nodules rests with their TiO_2 content, higher in the lavas than in the high-pressure xenoliths.

Mica

Trioctahedral micas (representative analyses are listed in Table 10) represent an important constituent of the lamproite mineralogy, from 15 to 30% in volume.

Two kinds of micas are present, some are authigenic crystals whereas others can be interpreted, with various degrees of certainty, as xenocrysts. In two specimens (73A8 and MC77) large independent crystals of phlogopite appear to have been destabilized, with abundant exsolution of needle-like Ti-rich phases. Analyses of these micas show tetrahedral site with 4.00 or close to 4.00 atoms, low TiO_2 (2 to 3%) and high Al_2O_3 (12 to 15%) contents, unusual values for lamproitic micas. These crystals are considered to be xenocrysts. Other large phlogopites may be found either as cores of complex micas, or have served as nuclei for lamproitic micas crystallization. They may (7B8, 5B6) or may not (74A1, 72A7, 7B8, 5B6, 8A12) appear unstable, with Ti-oxide exsolutions. Surrounding lamproitic micas are higher in Ti, Fe and lower in Al than the cores which show TiO_2 contents around 2%, and significant Cr_2O_3 percentages (from 0.30 to 1.0). Such high Cr_2O_3 contents have been recorded from peridotites (e.g., Boyd and Nixon, 1978; Delaney et al., 1980; Jones et al., 1982) or from phlogopite centers in some Monument Valley minettes (Jones and Smith, 1983). Typical lamproite micas plot near the phlogopite composition, the Fe/(Fe + Mg) ratio always below 0.30. They are often zoned concentrically, with an increase of both Ti and Fe and a concommitant decrease in Al from center to edge. They show a deficit in the tetrahedral site, Si + Al + Cr < 4 atoms.

Concerning the substitution in the tetrahedral site, several possibilities have been investigated. The presence of Fe^{3+} on the tetrahedral site of micas has long been known. Tetraferriphlogopite is found in nature (Cross, 1897) and has been synthesized in the laboratory. Silicon and magnesium can proxy for aluminum on the tetrahedral site (Seifert and Schreyer, 1971; Tateyama et al., 1974).

Robert (1981) showed (using infrared techniques) the presence of tetrahedral Mg in a Smoky Butte lamproite phlogopite. He was also able to demonstrate that this particular mica does not contain any Fe^{3+}, and that Ti is exclusively located on the octahedral sites.

Ti in micas. Various substitution mechanisms have been proposed to accomodate Ti in phlogopite. If Ti is fixed on the oc-

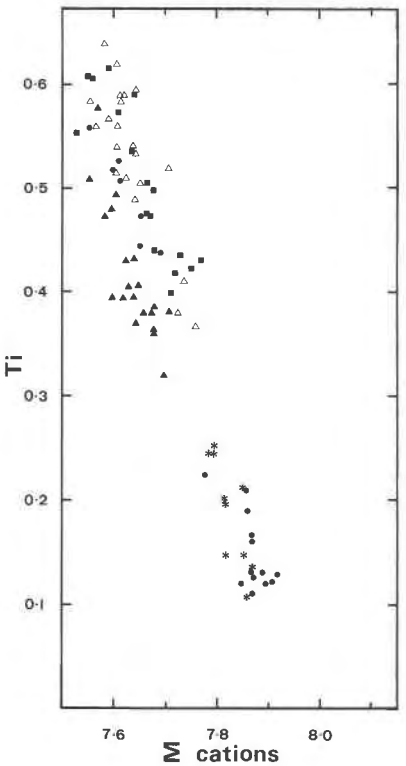

Fig. 7. The distribution of Ti and the sum of cations in phlogopites from 5 specimens. Solid triangles, 74A1; solid circles, 72A7; solid squares, 11A8; asterisks, 73A8; open triangles, 7B8.

tahedral site, it replaces a divalent ion, and hence all proposed mechanisms are coupled substitutions. These substitutions can be limited to the octahedral site or involve either one or two other structural sites. The various mechanisms proposed are as follows:

$2Mg = Ti + \square$	Forbes and Flower (1974)	(1)
$3Mg = Ti + Ba + \square$	Velde (1979)	(2)
$Mg + 2Si = Ti + 2Al$	Robert (1976)	(3)
$Mg + Si = Ti + Mg$	Robert (1976)	(4)
$Mg + 2OH = Ti + 2O$	Arima and Edgar (1981)	(5)

Substitution (1) was proposed after consideration of the composition of natural phlogopites, and has been recognized by Velde (1979) for micas found in melilite-bearing rocks where it is probably coupled with a substitution involving the incorporation of barium on the interlayer site. When this mechanism is operative a vacancy is created for every 2 Ti atoms entering the structure and the octahedral site occupancy decreases. The existence of substitution (1) is demonstrated in Figures 6 and 7 where Ti is related to the total number of ions. It is of course assumed that both the tetrahedral and interlayer sites are filled and that no Fe^{3+} is present in the structure. It appears that for specimens 5B6, 8A12, SO136 the slope of the line defined by the experimental points is close to the expected value, whereas in Figure 7 there are more vacancies than would be expected from substitution (1) alone.

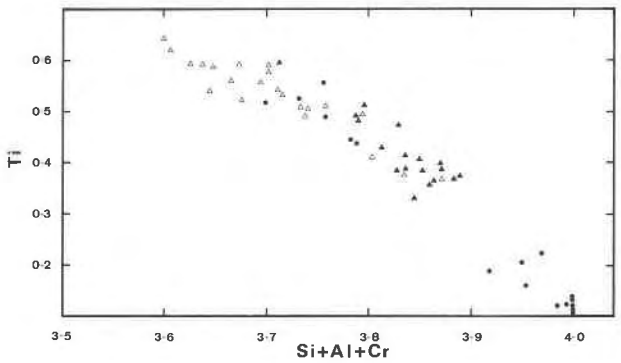

Fig. 8. The distribution of Ti and Si + Al + Cr in phlogopites from 3 specimens. Solid triangles, 74A1; solid circles, 72A7; open triangles, 7B8.

The incorporation of titanium on the octahedral site allows for the introduction of a divalent ion, magnesium (Robert, 1981) on the tetrahedral site (equation 4). In this case, a positive correlation would exist between Ti and Mg (on the tetrahedral site) and hence a negative correlation between Ti and Si + Al + Cr would ensue. Such a correlation is indeed observed for micas of specimens 74A1, 72A7, 11A8, 7B8, 8A12, SO136 (Figs. 8, 9 and 10) with Ti contents above 0.26 atoms per structural formula. Among those micas that do show a negative correlation three different groups can be distinguished: micas from the first group (74A1, 72A7 and 7B8) and the second group (8A12 and 11A8) show similar slopes of the line defined by the experimental points on Figures 8 and 9, but for a given Ti value the site occupancy by Si + Al + Cr of micas from the first group is higher than the occupancy shown for the second group. This difference is mostly due to a difference in Al content, the micas from the first group being richer in Al than micas of the second group. In the third type, which only includes specimen SO136, mica analyses plot along a slope different from that defined by the two other groups. Such a substitution scheme however implies an inverse correlation between Si and Ti that is apparent only in specimen 8A12 (Fig. 11) and, to a lesser extent, specimen 7B8.

There is no correlation between the number of Si + Al + Cr atoms and the Ti content when the number of Ti atoms is below 0.26, indicating a different substitution mechanism. Robert (1976) has proposed substitution mechanism (3) when the Ti content is

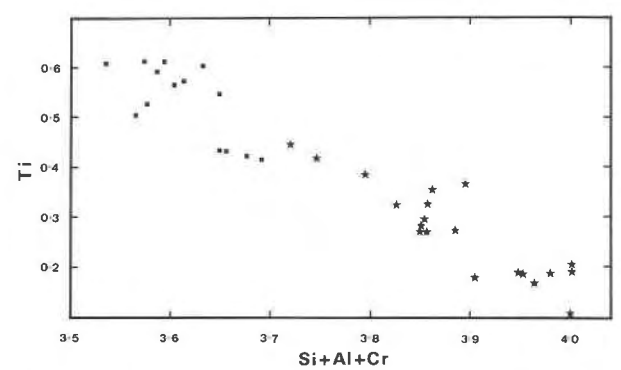

Fig. 9. The distribution of Ti and the sum Si + Al + Cr in phlogopites from specimens 11A8 (solid squares) and 8A12 (solid stars).

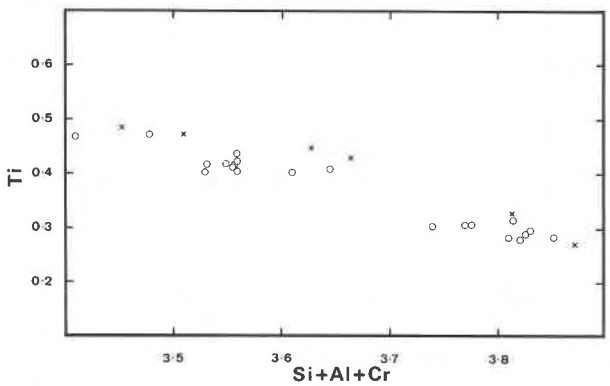

Fig. 10. The distribution of Ti and the sum Si + Al + Cr in phlogopites from specimen SO136 (open circles) and data from Mitchell (1981), crosses.

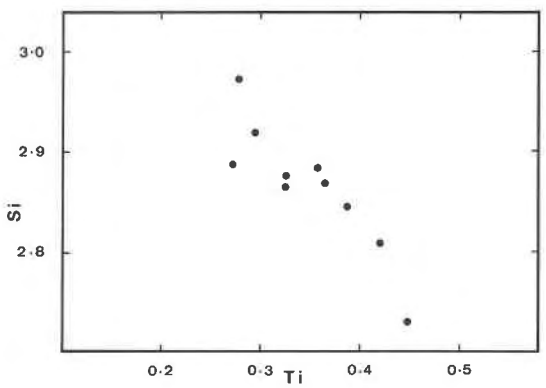

Fig. 11. The distribution of Si and Ti in phlogopites from specimen 8A12, analyses of crystal edges.

below 0.35. This substitution was looked for in analyses corresponding to the centers of micas from specimens 72A7 and 5B6 as well as for micas from 73A8 which show low titanium contents. The possibility of this substitution is confirmed by positive correlations between Ti and Al in all three cases.

In conclusion it seems that the most prominent substitution mechanisms for Ti in the micas studied are substitutions (1) and (4) for Ti-rich compositions. For Ti contents below 0.26 per structural formula the likely mechanisms are (1) and (3).

Interlayer ions. Ions in the interlayer site (K + Na + Ba) usually total close to the theoretical value of 1.0 atom per structural formula, the lowest value found being 0.85. Barium contents are low, usually below 1.0% BaO except for specimens 7B8 and 11A8 where it reaches 3%. This low barium content of micas in rocks where barium is abundant (see for example data for the Leucite Hills volcanics in Carmichael (1967), or as exemplified by the presence of Ba-rich phases in some lamproites such as priderite or barite) is probably due to the alumina-deficiency of the bulk composition. Most barium substitutions involve the mechanism Ba + Al = K + Si, an unlikely substitution in peralkaline rocks. In the lamproites examined the substitution appears to be of the kind Ba + □ = 2K. This vacancy-creating substitution could play a role, as does the possible vacancy-creating substitution for Ti. It should be pointed out that micas from specimens 7B8 and 11A8 show a correlation between Ti and Ba, with a different slope in each specimen.

Authigenic micas in lamproites differ from phlogopites from ultrabasic xenoliths by their high TiO_2 contents, but xenocrystic micas found in lamproites are similar, even in their trace element contents, with phlogopites from peridotites.

Table 11. Representative electron microprobe analyses of the roedderite-like phases, from Moon Canyon (analysis 1) and Cancarix (analysis 2). For comparison are listed analyses of roedderite (A, B) and eifelite (C) from Hentschel et al. (1980) and Abraham et al. (1983) respectively

	1	2	A	B	C
SiO_2	70.29	69.86	70.60	71.32	69.06
Al_2O_3		0.17	0.50	0.36	0.57
FeO°	12.60	9.83	5.80	0.49	0.19
MgO	11.44	13.90	15.70	17.86	15.47
MnO	0.23	0.21	0.21	0.31	0.53
TiO_2	0.02	0.21	0.07	0.07	0.03
Na_2O	0.04	0.25	1.80	5.29	8.07
K_2O	4.48	5.14	4.20	4.16	4.16
Total	99.08	99.57	98.88	99.79	98.05
Si	12.310	12.116	12.100	11.818	11.92
Al		0.035	0.101	0.070	0.08
Fe2+	1.845	1.426	0.831	0.068α	0.03
Mg	2.987	3.594	4.012	4.412	3.98
Mn	0.034	0.031	0.030	0.044	0.08
Ti	0.003	0.027	0.009	0.009	
Na	0.014	0.084	0.598	1.699	2.70
K	1.001	1.137	0.918	0.879	0.92

FeO°= Total iron as FeO

α : Fe 3+

1, Cancarix ; 2, Moon Canyon.

A, B : Hentschel et al., 1980.

C, Abraham et al., 1983.

Roedderite-like phases

Both the Cancarix and the Moon Canyon lamproites contain remarkable small prismatic crystals of a pleochroic blue mineral. Electron microprobe analyses of these blue minerals in both specimens have shown that they have similar compositions to minerals of the roedderite–eifelite series (Hentschel et al., 1980; Abraham et al., 1983). Representative analyses from Cancarix, Moon Canyon and of roedderite and eifelite are reproduced in Table 11. The roedderite-like minerals from the lamproites are distinct from those previously described in terrestrial rocks in their composition and in the fact that, for the lamproites, they are part of the mineralogical association, and apparently crystallized from the liquid. They are closely associated with feldspars, amphibole and late crystallizing micas. Their chemical compositions are different from that reported for the Eifel roedderites. The Cancarix mineral (a rare phase in the rock) is a sodium-free and iron-rich relative to the Eifel specimens. The Moon Canyon mineral (quite abundant in the specimen studied) is slightly less iron-rich, more magnesian and sodic than that from Cancarix. The lamproite minerals show a deficit in alkali metals for an R^{2+} total close to the theorical 5.0 value. Their general formula could be derived from the roedderite formula $(Na,K)_2Mg_5Si_{12}O_{30}$ through a substitution of the type $Fe^{3+} = Fe^{2+} + Na$. According to this scheme, the entry of Fe^{3+} in the structure creates one vacant site (an alkali site), the corresponding end-member being

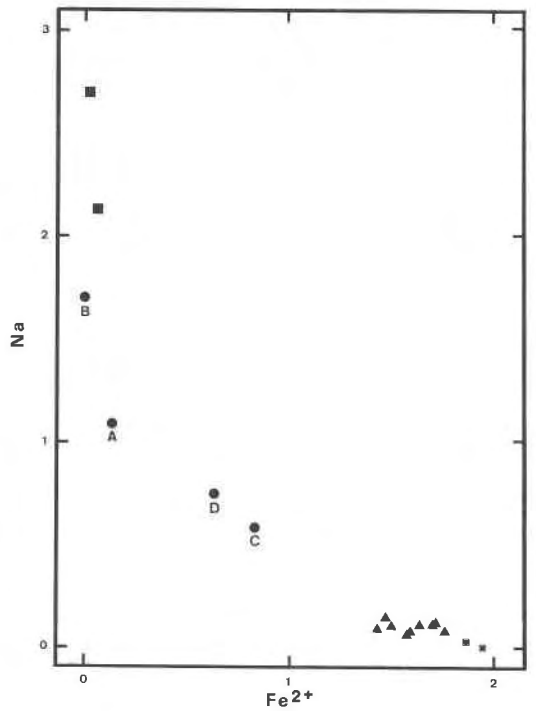

Fig. 12. The distribution of Na and Fe^{2+} in roedderite-like phases. Solid triangles, MC77; small solid squares, 74A1; solid squares, eifelites (Abraham et al., 1983); solid circles, roedderites (Hentschel et al., 1980).

$KFe^{3+}Fe^{2+}Mg_3Si_{12}O_{30}$. This substitution has been proposed by Hentschel et al. (1980) and Abraham et al. (1983) for roedderites found in the Bellerberg volcanic field of the Eifel in Germany. The Cancarix and Moon Canyon specimens are close to this theoretical end-member.

These relationships are demonstrated in Figure 12 which represents the variation of the Fe vs. Na. Na is absent, totally replaced by Fe^{3+}, in the Cancarix specimen. The iron-free eifelites plot along the horizontal axis, as they only show a 2Na = Mg substitution.

Table 12. Representative electron microprobe analyses of priderites from Australian, Sisco and Smoky Butte lamproites

	1	2	3	4	5	6	7
	SO136	SO136	7B8	7B8	7B8	8A12	8A12
Fe_2O_3°	10.97	9.19	9.53	9.09	7.66	10.75	9.59
MgO	0.92	0.74	1.15	1.02	0.76	0.17	0.03
TiO_2	76.17	72.89	70.43	68.18	66.60	71.46	70.83
Cr_2O_3	0.03	4.36	0.83	1.85	5.16		0.26
K_2O	6.82	7.15	2.56	2.73	2.67	2.27	1.37
BaO	5.43	6.30	16.22	16.73	16.93	16.39	17.08
Total	100.34	100.63	99.77	98.69	99.01	99.96	99.16
Fe3+	0.980	0.830	0.901	0.877	0.741	1.013	0.922
Mg	0.163	0.132	0.215	0.195	0.146	0.032	0.006
Ti	6.798	6.580	6.653	6.573	6.442	6.732	6.804
Cr	0.003	0.413	0.082	0.187	0.525		0.026
K	1.032	1.095	0.410	0.446	0.438	0.363	0.223
Ba	0.252	0.296	0.798	0.840	0.853	0.803	0.853
Total	9.227	9.346	9.060	9.118	9.144	8.943	8.834

Fe_2O_3° = Total iron as Fe_2O_3

Table 13. Representative electron microprobe analyses of pseudobrookites from various lamproites studied. Fe^{3+} calculated assuming 3 cations and 5 oxygens

	1	2	3	4
	74A1	73A8	7B8	MC77
Al_2O_3	0.02	0.47	0.30	0.06
Cr_2O_3	0.82	0.43	0.99	0.05
FeO°	28.97	19.66	19.86	23.46
MgO	8.65	9.39	8.92	7.61
MnO	0.33	0.15	0.14	0.20
TiO_2	60.33	69.02	69.04	66.32
Total	99.12	99.12	99.25	97.70
Fe_2O_3	26.38	8.57	7.71	11.03
FeO	5.24	11.94	12.92	13.54
Al	0.001	0.020	0.013	0.003
Cr	0.023	0.012	0.028	0.001
Fe3+	0.714	0.232	0.209	0.307
Fe2+	0.157	0.359	0.390	0.419
Mg	0.464	0.504	0.480	0.420
Mn	0.010	0.005	0.004	0.006
Ti	1.631	1.868	1.875	1.844

FeO° = Total iron as FeO

The deep blue color of the roedderite-like phase appears to be related to the presence of ferric iron in the structure. The Cancarix mineral, richer in iron (total iron) than the Moon Canyon one, has a deeper blue color. Hentschel et al. and Abraham et al. pointed out that their roedderites C and D, with 5.8 and 4.45% total FeO show a blue color.

Roedderite appears among the low-pressure breakdown products of richterite (Gilbert et al., 1982) and testifies to the strongly peralkaline character of these two lamproites.

Oxides

Titanium-rich oxides are a general feature of lamproites, as pointed out by Scott Smith and Skinner (1984). In this respect, lamproites differ from peralkaline siliceous rocks that are known for the absence of oxides (Carmichael, 1967). Besides chromites found as inclusions in olivine (considered below) these rocks contain one type of Fe–Ti oxide: ilmenite (11A8), or an association of two oxides: ilmenite + pseudobrookite (MC77 and 73A8); ilmenite + titanomagnetite (5B6); ilmenite + priderite (SO136, Sisco); pseudobrookite + priderite (7B8). These minerals and mineral associations are uncommon and will be described in some detail.

Priderite has been found and analyzed (Table 12) in rocks from Sisco, and Smoky Butte besides the Australian type locality. The original priderite contained 0.32 atoms of Ba and 0.87 atoms of potassium. Carmichael (1967) gave two electron microprobe analyses of priderites from the Leucite Hills and Australia. The priderites from Smoky Butte (where priderite is present in Type 1 lamproite, as noted by Velde (1975) but has also been found in specimen 7B8) are particularly Ba-rich, and the Ba content can reach 0.85 atoms, whereas K is only 0.4 per structural formula calculated on 16 oxygens. These high Ba-values imply, as hypothesized by Post et al. (1982), the existence of a Ba end-member of the priderite series. Another striking variation in the analyzed

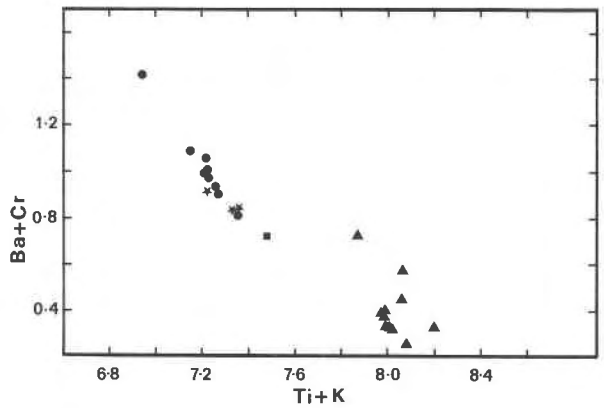

Fig. 13. The distribution of Ba + Cr and Ti + K in priderites. Solid circles: 7B8; solid stars: 8A12; solid triangles: SO136; solid square: LH9, Carmichael (1967).

priderites is their Cr-content: the priderites found in the Australian specimen may contain 4.36% Cr_2O_3, the minimum found being 0.03. The Cr_2O_3 content of the Smoky Butte priderite reaches 5.16%. The general formula of priderite (Norrish, 1951), $A_{2-y}B_{8-z}O_{16}$, is not adequately known, but it seems that the variations observed in the three lamproites mentioned are compatible with a substitution of the type:

$$Cr^{3+} + Ba^{2+} = Ti^{4+} + K^{+} \qquad \text{(Fig. 13)}$$

This scheme does not however account for the observed variation in the iron content, which could be at least partly in the ferric state and consequently participate in the above equation.

The presence and abundance of *pseudobrookite,* a rare mineral in terrestrial rocks, is peculiarly common to some of the lamproites studied. Pseudobrookite usually forms euhedral plates, hexagonal in shape, opaque or barely translucent in transmitted light. When translucent (as in Smoky Butte) crystals can appear either green or purple brown a difference that does not appear to be simply related to compositional variations. In specimen MC77 pseudobrookite appears as transparent golden brown crystals, with optical properties very close to those of rutile. In reflected light, these pseudobrookite crystals show reddish internal reflections. The composition of these oxides is 40% ferropseudobrookite, 12 to 15% pseudobrookite and 42 to 48% karrooite. Representative analyses are listed in Table 13. Specimen 73A8 contains pseudobrookite crystals, interpreted as xenocrysts which are extremely rich in magnesium (up to 52 mole% of the karrooite component). This particular pseudobrookite is close in composition to armalcolite (Anderson et al., 1970; Haggerty, 1973; El Goresy and Bernhardt, 1974). Pseudobrookite has been found, as a primary mineral, in few terrestrial rocks: in meteorite impactites (El Goresy and Chao, 1976), in kimberlites (Haggerty, 1975; Raber and Haggerty, 1979), in ultrabasic nodules (Cameron and Cameron, 1973) and lamproites (Velde, 1975). It has also been found in some basalts (Anderson and Wright, 1972; Van Kooten, 1980; Von Knorring and Cox, 1961), and in meteorites (Fujimaki et al., 1981). It was described by Rice et al. (1971) as a quenched mineral in a dike rock of basaltic composition. According to Haggerty (1976), the presence of primary pseudobrookite implies a fast cooling rate that prevents a reaction of the pseudobrookite with the liquid, a reaction whose end product would normally be ilmenite. It should be pointed out that in no lamproite was any ilmenite rim found around the early-formed pseudobrookite.

Ilmenite is accompanied by priderite in specimen SO136 where priderite forms abundant small elongated crystals, as well as in some of the Sisco specimens (Velde, 1968) where it is quite rare. Ilmenite forms small crystals (5 to 50 μm maximum) without evidence of exsolution or oxidation, except for specimen 74A1. Ilmenites appear after olivine, diopside and the centers of the phlogopites crystals. They are usually poor in hematite, containing from 64 to 90% of the ilmenite component, 11 to 30% geikelite and 1 to 2% pyrophanite. Representative analyses are listed in Table 14.[1] Specimen 73A8 contains probable xenocrysts of a magnesian ilmenite with a rutile core; the composition of the ilmenite is similar, though not as Mg-rich, to that of xenocrystic Mg-ilmenites described by McMahon and Haggerty (1984), a composition close to the composition of ilmenites found in kimberlites (Dawson, 1980).

Chromites (Table 3) found as inclusions in authigenic olivines are similar by their high Cr_2O_3, low Al_2O_3, and high Mg/(Mg + Fe) to chromites found by Danchin and Boyd (1976) in harzburgites, themselves, as pointed out by these authors, not unlike chromites found as inclusions in diamonds. Their low Al is in keeping with the peralkaline chemistry of the magma, their high Cr could be related to the low Al and Fe^{3+} contents of the liquid.

Ti-rich oxides are commonly abundant in peralkaline lamproites. This presence and abundance could be ascribed to the high TiO_2 and high FeO contents of these rocks. When projected in an FeO–Fe_2O_3–TiO_2 diagram the composition of most pseudobrookite (+ ilmenite) bearing samples plot close to the ferropseudobrookite-pseudobrookite line or do so when the amount of iron (and TiO_2) partitioned in the early-crystallized silicates is taken into account.

Most of the oxides do not show any exsolution or oxidation textures and most compositions can be recalculated into ferrous, rather than ferric, end-members, or minerals with high ferrous iron contents. This observation is taken as an indication of the low oxygen contents of the melts, compatible with the low Fe^{3+}/Fe^{2+} ratio of most ferromagnesian silicate phases present in these lavas.

Oxides are known to occur with phlogopite and richterite in ultrabasic nodules, rutile and ilmenite being common, pseudobrookite rare.

Conclusion to the mineralogical description

Lamproites described above can be considered as presenting a magmatic assemblage consisting of Al-poor, Cr-rich spinel, Ni-rich olivine, Ti-phlogopite, Ti-rich K-richterite, diopside, Fe-rich feldspar and Ti-rich oxides. Olivine crystals having evident textural (kink-bands) analogies with peridotitic olivines are also found and can be interpreted as being inherited from the solid layers of the earth through which the lamproitic magma percolated. Other such inherited minerals are Cr-rich diopsides, Fe-rich clinopyroxenes, Cr-rich phlogopites, pseudobrookites, Mg-ilmenites and large rutile crystals (accidental in some Spanish lamproites). Jones and Smith (1983) have also demonstrated the presence, in the Navajo minettes, of apatite and clinopyroxenes xenocrysts. The possible presence of various xenocrystic species in the Leucite Hills lavas was also discussed by Kuehner et al. (1981) who, for example, described pleonaste in the Deer Butte wyomingite.

Hence care should be exercised before discussing either

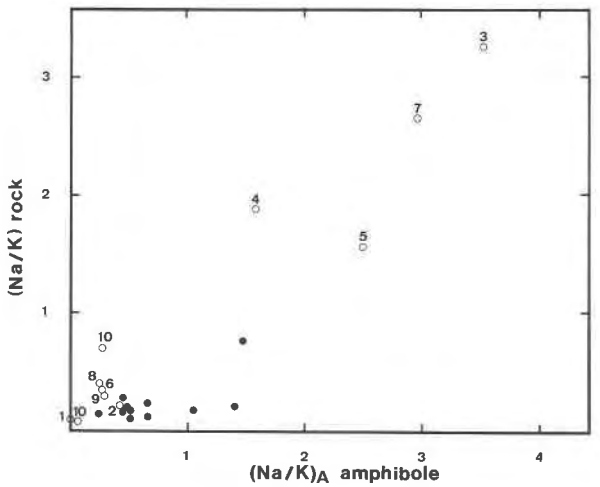

Fig. 14. The distribution of Na/K calculated from the bulk rock composition and the Na/K content of the A site of the richterite. Solid circles: data from this study; open circles: data from the literature: 1, LH9, Carmichael (1967); 2, Type 1, Velde (1975); 3, Velde (1978); 4, S84, Bryan (1970); 5, RH1, Barker and Hodges (1977); 6, Brooks et al. (1978); 7, 121, Nicholls and Carmichael (1969); 8, Sheraton and England (1980); 9, S1, Carmichael (1967); 10, Jaques et al. 1984.

the partitioning of elements between phases or the significance of the trace element geochemistry of these rocks.

Partitioning of elements between phases

Some elements are found in certain phases in proportions which can be correlated with the bulk rock composition. The Fe^{3+} content of the feldspar is simply correlated with the peralkalinity index of enclosing rock. Micas are more potassium rich in the most potassium rich bulk composition, a relation already described by Edgar and Arima (1983). Richterites contain variable amounts of potassium and there is a relationship between the potassium content of the richterite and the amount of potassium present in the rock expressed in the form of the

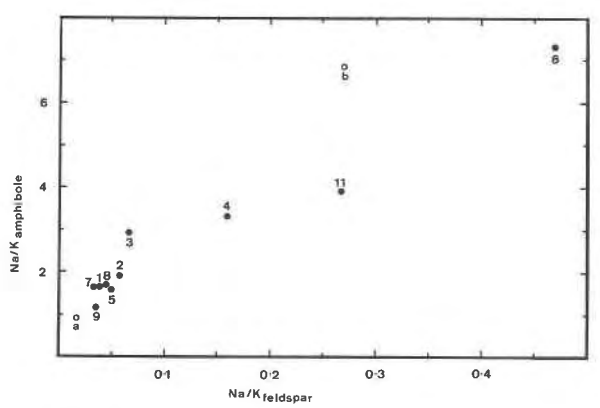

Fig. 15. Partitioning of Na and K between richterites and feldspars. Data from this study: solid circles; data from the literature: open circles (a, LH9, Carmichael, 1967; b, Velde, 1978).

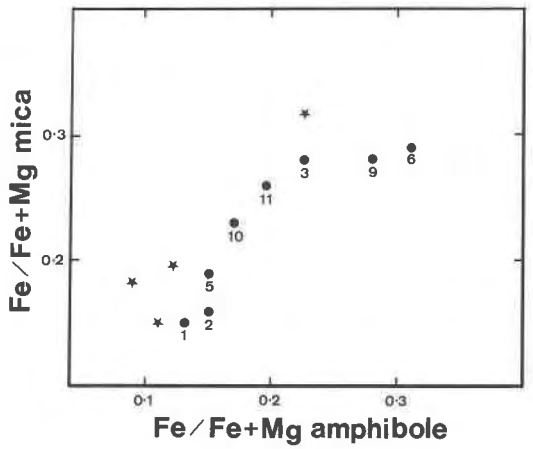

Fig. 16. Partitioning of Fe and Mg between phlogopites and richterites. Data from lamproites: solid circles; data from ultramafic nodules (Aoki, 1974, 1975; and Dawson and Smith, 1977): solid stars.

Na/K ratio. Figure 14 shows this correlation, as deduced from specimens under consideration and examples taken from the literature. Richterites also appear to be more potassic when the rock is more peralkaline, which could be another way of expressing the previous correlation, the peralkalinity in lamproites being directly related to the potassium content.

This being established, how are these elements distributed between co-crystallizing phases? Since richterite and phlogopite coexist in some ultrabasic nodules brought to the surface by kimberlitic magma, these nodules represent physical conditions different from those of lamproitic crystallization, in particular different pressure conditions. These data have been included in Figures 16 to 18. In

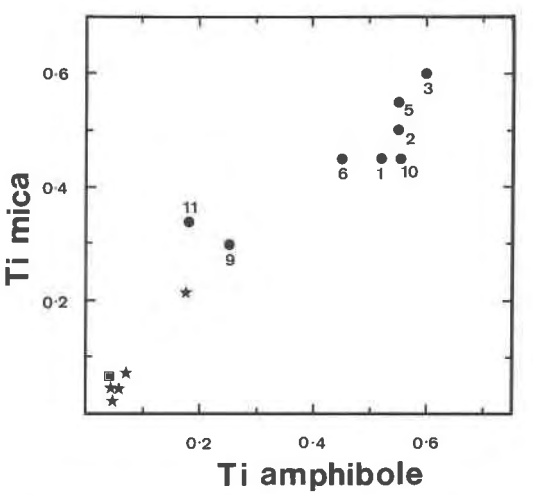

Fig. 17. Partitioning of Ti between micas and richterites. Data from lamproites: solid circles; data from nodules: solid stars (Aoki, 1974, 1975; and Dawson and Smith, 1977) and solid squares (data from Jones et al., 1982).

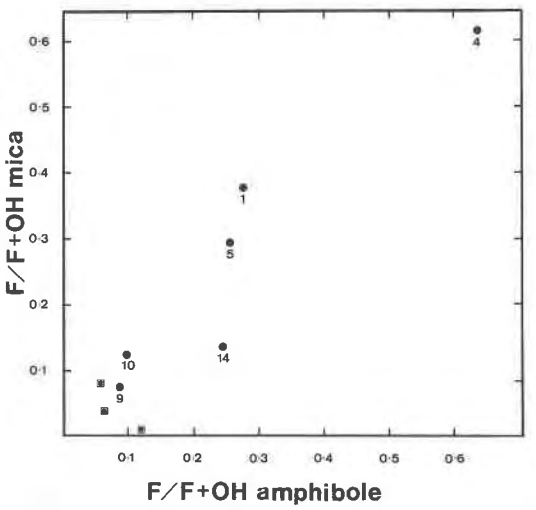

Fig. 18. Partitioning of fluorine between phlogopites and richterites. Data from lamproites: solid circles; data from nodules (Jones et al., 1982): solid squares.

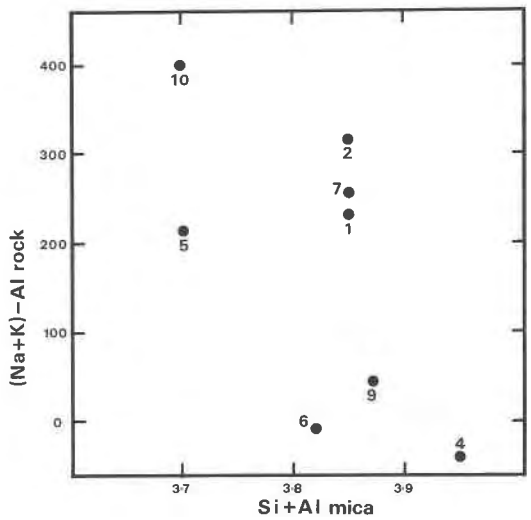

Fig. 20. The distribution of (Na + K) − Al calculated from the rock bulk compositions and the Si + Al content of the phlogopites.

this way the influence of pressure on the composition of the minerals under consideration can be evaluated.

Sodium and potassium: there is a direct relationship between the Na/K ratio of richterite and the coexisting feldspar (Fig. 15).

Iron is equally distributed between amphibole and phlogopite (Fig. 16) in lamproites as well as in ultrabasic nodules found in kimberlites but this is only valid when considering those micas and amphiboles in equilibrium, judged so on the basis of textural arguments (Table 15[1]).

There is a positive correlation (Fig. 17) between Ti in micas and amphiboles. It should be noted that the localization of titanium in the amphibole structure is still ambiguous, and that the problem, for micas, cannot be considered as unambiguously solved even if Ti is probably incorporated on the octahedral site in lamproite micas. Lower Ti-contents appear to characterize micas and amphiboles from ultrabasic nodules.

Fluorine: the maximum content of fluorine found in a natural mica is 8.5% (Peterson et al., 1982; Valley et al., 1982) and 4.5% in a natural richterite (in a meteorite, Olsen et al., 1973). Synthetic minerals contain up to 9.2% F for phlogopites (Kohn and Hatch, 1955) and 4.7% in richterite (Kohn and Comeforo, 1955). In lamproite phlogopites the fluorine content is, in most cases, below 1%, but can reach 4% (specimen 73A8). These F contents are in agreement with what can be calculated from the F content of the rock and the modal amount of phlogopite, with the exception of specimen 11A8, a rock particularly rich in F-bearing apatite. Representative analyses of F-rich micas and amphiboles from lamproites are listed in Table 16.[1]

Figure 18 seems to indicate that F is equally distributed

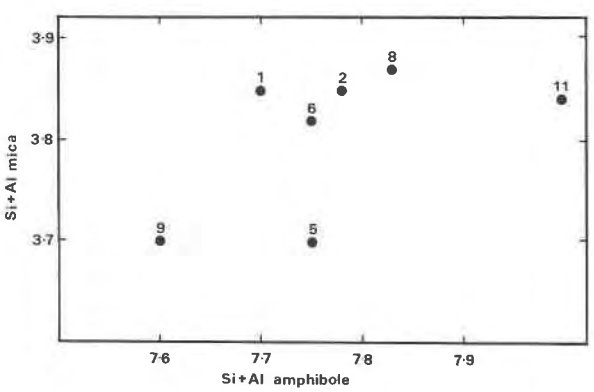

Fig. 19. The distribution of Si + Al in phlogopites and richterites.

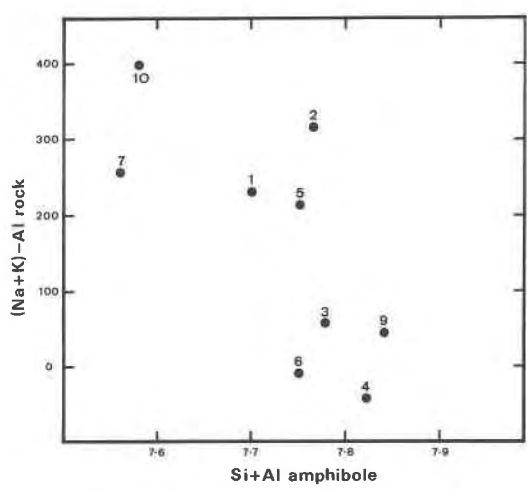

Fig. 21. The distribution of (Na + K) − Al calculated from the rock bulk compositions and the Si + Al content of the richterites.

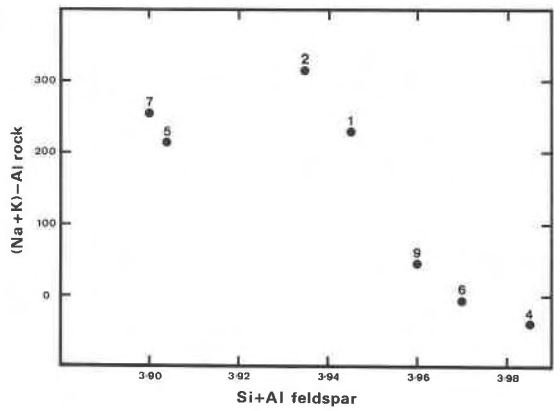

Fig. 22. The distribution of (Na + K) − Al calculated from the rock bulk compositions and the Si + Al content of the coexisting feldspars.

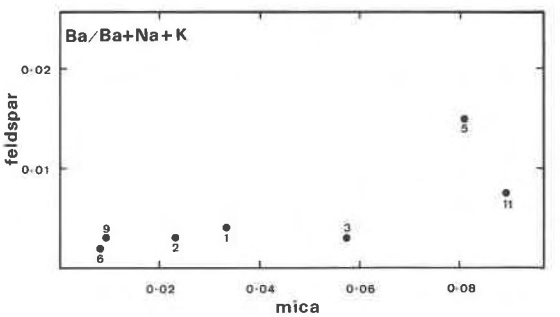

Fig. 23. The distribution of Ba/(Ba + Na + K) in feldspar and coexisting mica.

(K_D = 1) between the two phases phlogopite and richterite (Table 15). It should be pointed out that the diagram includes values for specimen 73A8 in which the two phases are not considered to be in equilibrium (textural evidence); their F values follow the same trend as that determined for phases thought to be in equilibrium. This observation could be interpreted as indicating that F and OH can equilibrate after crystallization of the two phases. The K_D values calculated using the F determinations published by Jones et al. (1982) for mica and amphibole pairs in metasomatized peridotites are widely different from one another and from those given here. This anomaly cannot be explained at present. Note should be made of the fact that, in the Spanish lamproites, phlogopites show a distinct correlation between F and Ti. This correlation was found in richterites only from specimens 74A1, 73A8 and 7B8.

Si + Al on the tetrahedral sites: most of the phases present in the peralkaline lamproites do not contain enough Si + Al to fill the tetrahedral site to its theoretical number of ions. This point was discussed in the preceding section and, in all cases, the nature of the other ion (ions) could not be decided upon with the data at hand.

In spite of the unknown nature of the supplementary ion (or ions) on the tetrahedral site it is interesting to note that the amplitude of this Si + Al deficiency is similar in the coexisting minerals within a given specimen. Figure 19 shows the relationship between the value of Si + Al in the micas and in the coexisting amphibole. There is a positive correlation between the tetrahedral Si + Al content of both phases. Because tetrahedral deficiency appears to be linked to the peralkalinity of the liquid, the Si + Al content of various phases has been plotted against the (Na + K) − Al value of the corresponding bulk composition (Figs. 20 to 22). The apparent correlation is not valid for the Jumilla specimen, already commented upon.

Barium is preferentially incorporated in micas (Higuchi and Nagasawa, 1969; Wörner et al., 1983) but is also present in coexisting feldspars. The distribution of Ba between feldspar and mica in the lamproites is regular as shown on Figure 23. Data from Wörner et al. (1983) indicate that BaO contents in phlogopites are twice the BaO contents in associated sanidines. Three specimens show K_D's for Ba between feldspar and mica that are quite comparable: 0.196 (7B8), 0.192 (74Al) and 0.175 (72A7) but low when compared to values found in other types of volcanic rocks.

Most elements are regularly partitioned between coexisting amphiboles and phlogopites. The bulk composition (either iron, magnesium or titanium contents) exerts some control on the corresponding contents of the minerals in these elements. The silica saturation is however not an important factor in the control of the mineral compositions, whereas aluminum saturation, on the contrary, is a determinant factor particularly on the content of the tetrahedral site.

Temperature estimations of cooling history

A number of experimental studies have been made on either phlogopites, richterites or oxides. These data can tentatively be used to estimate temperature of crystallization.

Initially a spinel–olivine geothermometer (Sack, 1982) can be used. The authigenic rim around olivine xenocrysts from the Calasparra lamproite give 1000°C (72A7) whereas the olivines from the rock give 800°C. The selagite spinel-olivine associations give values between 914 and 1160°C, whereas a 1000°C phenocryst temperature has been calculated for the jumillite (11A8). In this specimen an olivine coexisting with glass inside an apatite crystal gave a high crystallization temperature of 1221°C with the method outlined by Watson (1979).

The maximum thermal stability of the lamproite amphiboles is between 985 and 1030°C (Charles, 1975, 1977) taking into account only the Mg–Fe substitution. Richterite is more stable when it is more magnesian and Barton and Hamilton (1978) have shown that a richterite from the Leucite Hills was stable up to 1075°C at H_2O pressures of 1 kbar. A crystallization temperature, based upon the partitioning of Na and K between amphibole and liquid, has been calculated for two specimens (Smoky Butte and Jumilla) where amphibole and coexisting glass composi-

tions were known, using the relation established by Helz (1979): the values found are 965°C for Smoky Butte and 770°C for Jumilla.

Attempts to estimate temperature of crystallization using the oxide phases were obviously hindered by the absence of magnetite and by possible secondary oxidation. However one sample (specimen 5B6) contains coexisting ilmenite and titanomagnetite which show neither oxidation nor exsolution. These oxides have appeared early in the crystallization sequence, judging from textural relationships, after clinopyroxene. While titanomagnetite appears homogeneous, there is a variation in the Fe_2O_3 of the ilmenites which decreases from the center towards the rims of the crystals. Using a program published by Ghiorso and Carmichael (1981), two sets of temperatures were obtained: for the centers of the ilmenites and the magnetites the calculated temperature is 827°C for a log $fO_2 = -13.5$ whereas considering the edges of the ilmenites the calculated crystallization temperature is 755°C for log $fO_2 = -15$. These results are similar to those deduced from the phase diagrams published by Haggerty (1976).

These temperature estimations for various minerals or mineral pairs allows one to establish the following:

(1) Xenocrysts with included spinels were not found. Olivine xenocryst rims crystallized at temperatures of 1000–1200°C.

(2) Groundmass olivine crystallized at 800–900°C.

(3) Amphiboles formed at temperatures between 960 and 770°C.

(4) When ilmenite and magnetite are present (Shiprock) temperatures between 800–700°C are indicated.

These values pertaining to a range of lavas with differing compositions are in broad agreement with the liquidus determinations of Carmichael (1967) who found 1165° and 1200°C for two different wyomingites. The data published by Barton and Hamilton (1978) also for wyomingites, in water-saturated conditions, are in general agreement with the crystallization order found here.

High pressure–low pressure phases. A comparison should now be made with mineral composition recorded from ultrabasic inclusions. Common characteristics between richterites found in nodules and richterites found in lamproites are the following: their potassium content is similar, as is Na/K, their tetrahedral site is incompletely filled by Si and Al atoms, but Fe^{3+} is present in amounts great enough to saturate the tetrahedral site. These richterites can be distinguished from those found in lamproites by a lower TiO_2 content (less than 0.1 Ti atoms per structural formula). Kushiro and Erlank (1970) have obtained recrystallization at 1100°C and water pressure of 30 kbar of a potassic richterite close in composition to the Australian richterite used as starting material, except for TiO_2 content: the TiO_2 content of the starting material was 3%, whereas the artificial richterite contained only 0.5% TiO_2. This result implies that the entry of titanium in the richterite structure is favored by low pressure.

Phlogopite, as well as richterite, is an important constituent of some of the nodules found in kimberlites and both minerals have been found as inclusions in diamonds (Meyer and McCallum, 1984). Phlogopite-bearing nodules are more frequent than nodules carrying both phlogopite and richterite. These phlogopites (Dawson and Smith, 1977; Aoki, 1974, 1975) contain less Ti than the phlogopites found in lamproites (less than 0.1 atoms per structural formula), but they also show a tetrahedral site incompletely filled by Si + Al.

The influence of titanium on the stability of micas is not precisely known. Forbes and Flower (1974) envisioned that Ti stabilized the phlogopite; Robert (1981) and Robert and Chapuis (1982) have considered Ti-rich micas as high-pressure phases and this hypothesis is also accepted by Bachinski and Simpson (1984) who consider the Ti-rich (2.0 to 11.3% TiO_2) cores of minette phenocrysts to have crystallized at elevated subcrustal pressures. However, Edgar et al. (1976) established that between 10 and 30 kbar Ti-poor phlogopite is stable relative to Ti-rich phlogopite. Wendlandt and Eggler (1980) have furthermore shown that the Ti content of the phlogopite decreased with pressure for identical compositions, a proposition confirmed by Arima and Edgar (1981). All lamproite micas considered in the present study, excepting xenocrysts, have crystallized at low pressures being found in rocks that have solidified at the surface. Consequently, Ti-rich phlogopites and amphiboles crystallize under pressures corresponding to the surface of the earth. The absence of Ti-rich phlogopites in kimberlite nodules, in assemblages that, for the most part, include Ti-oxides could be interpreted as meaning that Ti-phlogopite is not stable at high pressure.

Discussion and conclusions

K-Ti-richterites and Ti-phlogopites are the prominent minerals found in peralkaline lamproites. They commonly coexist with Ti-rich Fe-Ti oxides and may be accompanied by rare alkali-rich phases such as priderite, or roeddderite-like minerals. These associations testify to the peralkaline composition of the liquids from which these minerals precipitated. Coexistent with, but genetically unrelated to this magmatic association, are found a number of phases that have been scavenged by the ascending lamproitic magma. These phases are the same species as those precipitating from the lamproitic magma, i.e., olivine, clinopyroxene, trioctahedral mica, ilmenite, pseudobrookite, rutile and apatite. The rate of dissolution being governed by the minerals stable on or close to the liquidus (Brearley and Scarfe, 1984). The volumetric importance of these relics is not considerable (less than 10%) but, taking into account experiments performed by Scarfe et al. (1980) on basalts, material might have been dissolved into the liquid. Incorporation of Ni-rich olivines at depth could, for example, account for the precipitation of Ni-rich olivines from the magma at the surface; incorporation of Cr-rich phases for the precipitation of Cr-diopside or Cr-rich spinels.

Results of the present study show that peralkalinity of

lamproites is a characteristic of the lamproitic liquid, because of the correlations between some mineral compositions and the alkalinity index, or the precipitation of Al-poor chromite as a liquidus phase. Hence contamination during the ascent of the magma cannot account for the high alkali (potassium) and low Al contents.

Partitioning of elements between phases, excluding xenocrysts, is regular and follows trends in keeping with those that can be deduced from mantle metasomatic assemblages of phlogopite and richterite. A conclusion is that the high K-richterites found in mantle xenoliths are probably derived from the reactions of highly potassic fluids with ultrabasic rocks. The difference between Ti contents of phlogopite and richterite in lamproites (low pressure) and metasomatized peridotites (high pressure) reflects the higher solubility of Ti in these phases at low pressure.

A deep seated origin of these liquids is suggested by two series of observations:

The presence of peridotite xenoliths known to occur in the Leucite Hills (Carmichael, 1967; Barton and Bergen, 1981), in the Australian lamproites (Jaques et al., 1984) and in the Spanish lamproites (Velde, 1969; Nixon et al., 1982).

The discovery of diamonds in a number of Australian lamproite localities (Jaques et al., 1984). This observation alone places the lamproites in a category of rocks akin to kimberlites, at least for the depth at which they originate. Trace element data, and in particular rare earth profiles, when available, indicate for lamproites, as for kimberlites, an extreme enrichment in light rare earth elements (500 to 2000 the chondritic values), and a weaker enrichment in heavy rare earth (Nixon et al., 1982; Mitchell and Hawkesworth, 1984).

The bulk composition of lamproites is so different from common magmatic rocks that their deviation from, for example, basaltic magmas is not permitted. As pointed out by Carmichael (1967) when considering the genesis of the Leucite Hills volcanics, the temptation is to impose on the starting material many of the requirements of the result that is supposed to be achieved. Since Carmichael's study, however, the concept of mantle metasomatism has been widely commented upon (Bailey, 1982). Ultrabasic rocks have been described with a metasomatic assemblage resulting from the reaction of mantle associations with K-rich fluids (Jones et al., 1982; Barton and Hamilton, 1982) that could be precisely the source of ultrapotassic peralkaline rocks.

It is tempting to pursue this reasoning and calculate what percentage of the bulk compositions of lamproites can be explained with the fusion of a richterite–phlogopite–rutile (or ilmenite)–diopside assemblage. Least square calculations performed using the compositions of these phases as listed by Dawson (1980, p. 186) lead to the following conclusions: all the bulk compositions of lamproites listed in Table 2 can be obtained by the fusion of the above kimberlitic nodule assemblage. In all cases, required percentages of phlogopite are between 50 and 70% (weight), but most cluster between 56 and 68%. Required percentages of richterite vary between 30 and 50%, except for Jumilla, whose bulk composition has been altered and will not be considered further, Shiprock and the Australian lamproite. In these two last samples, diopside must be included in the starting material. In all calculations rutile is added, the proportions being above 1% (weight) only for the most titaniferous compositions, Smoky Butte and Australia. Recent experiments (Dickinson and Hess, 1984) have indeed shown that the solubility of rutile (K*) increases dramatically with the $K_2O/K_2O + Al_2O_3$ of the liquids, from 9.5 wt.% (K* = 0.37) to 41.2 wt.% (K* = 0.90).

For the calculated values to match the observed lamproite compositions, fractionation of olivine, and clinopyroxene, and a certain alkali loss must be called for.

The fact that lamproite major elements compositions can be matched in such a fashion cannot be considered as proof of a particular genetic process. The coincidence simply permits this scheme to be used as a working hypothesis for a more rigourous treatment of the problem that would include data on trace elements combined with the precise determination and evaluation of xenocrystic material that could further constrain the problem.

Acknowledgments

John Hower gave Danielle Velde, in 1968, three samples from Smoky Butte, Montana; preliminary work on these specimens prompted a visit to this locality, but large parts of this study ensued from this gift. The first specimen obtained from Moon Canyon was generously given by M. G. Best, Brigham Young University; the subsequent ones were forwarded to us through the courtesy of Professor Blanchet, from the University of Brest. The Australian specimen was obtained through Dr. Esquevin, S.N.E.A.P., Pau. Professor A. Baronnet and J. Fabriès reviewed parts of this manuscript at various stages of its preparation, Professor W. Schreyer (University of Bochum) confirmed us in the opinion that our "roedderite" was probable a new mineral, and Dr. A. El Goresy (Max Planck Institut, Heidelberg) was most helpful in helping to decipher the complex relationships between opaque phases.

References

Abraham, K., Gebert, W., Medenbach, O., Schreyer, W., and Hentschel, G. (1983) Eifelite, $KNa_3Mg_4Si_{12}O_{30}$, a new mineral of the osumilite group with octahedral sodium. Contributions to Mineralogy and Petrology, 82, 252–258.

Anderson, A. T., Bunch, T. E., Cameron, E. N., Haggerty, S. E., Boyd, F. R., Finger, L. W., James, O. B., Keil, K., Prinz, M., Ramdohr, P., and El Goresy, A. (1970) Armalcolite: a new mineral from the Apollo 11 samples. Proceedings of the Apollo 11 Lunar Science Conference, 1, 55–63.

Anderson, A. T. and Wright, T. L. (1972) Phenocrysts and glass inclusions and their bearing on oxidation and mixing of basaltic magmas, Kilauea Volcano, Hawaii. American Mineralogist, 57, 1–188.

Aoki, K. (1974) Phlogopites and potassic richterites from mica nodules in South African kimberlites. Contributions to Mineralogy and Petrology, 48, 1–7.

Aoki, K. (1975) Origin of phlogopite and potassic richterite bearing xenoliths from South Africa. Contributions to Mineralogy and Petrology, 53, 145–156.

Aoki, K., Ishiwaka, K., and Kanisawa, S. (1981) Fluorine geochemistry of basaltic rocks from continental and oceanic regions and petrogenetic applications. Contributions to Mineralogy and Petrology, 76, 53–59.

Arima, M. and Edgar, A. D. (1981) Substitution mechanisms and solubility of titanium in phlogopites from rocks of probable mantle origin. Contributions to Mineralogy and Petrology, 77, 288–295.

Armstrong, R. L. (1969) K–Ar dating of the laccolitic centers of the Colorado Plateau and vicinity. Bulletin of the Geological Society of America, 80, 2081–2086.

Bachinski, S. W. and Simpson, E. L. (1984) Ti-phlogopites of the Shaw's Cove minette: a comparison with micas of other lamprophyres, potassic rocks, kimberlites, and mantle xenoliths. American Mineralogist, 69, 41–56.

Bailey, D. K. (1982) Mantle metasomatism. Continuing chemical change within the earth. Nature, 296, 525–530.

Barberi, F. and Innocenti, F. (1967) Le rocce selagitiche di Orciatico e Montecatini in Val di Cecina. Atti Societa Toscana Scienze Naturali, Memorie Serie A, LXXIV, 139–180.

Barbot, J. (1983) Le nickel dans les olivines et les spinelles des roches basiques et ultrabasiques. Thèse 3ème cycle, Université de Bretagne Occidentale.

Barker, D. S. and Hodges, F. N. (1977) Mineralogy of intrusions in the Diablo Plateau, northern Trans-Pecos magmatic province, Texas and New Mexico. Bulletin of the Geological Society of America, 88, 1428–1436.

Barton, M. and Bergen, M. (1981) Green clinopyroxenes and associated phases in a potassium rich lava from the Leucite Hills, Wyoming. Contributions to Mineralogy and Petrology, 77, 101–114.

Barton, M. and Hamilton, D. L. (1978) Water-saturated melting relations to 5 kbar of three Leucite Hills lavas. Contributions to Mineralogy and Petrology, 66, 41–49.

Barton, M. and Hamilton, D. L. (1982) Water-undersaturated melting experiments bearing upon the origin of potassium rich magmas. Mineralogical Magazine, 45, 267–278.

Bellon, H. (1976) Séries magmatiques néogènes et quaternaires du pourtour de la Méditerranée occidentale, comparées dans leur cadre géochronométrique—Implications dynamiques. Thèse Doctorat d'Etat, Université Paris-Sud.

Bellon, H. (1981) Chronologie radiométrique (K–Ar) des manifestations magmatiques autour de la Méditerranée occidentale entre 33 M.A. et 1 M.A. Proceedings International Conference, Urbino University, Italy, 341–360.

Bellon, H., Bizon, G., Pedro-Calvo, J., Gaudant, J., and Lopez-Martinez, N. (1981) Le volcan du Cerro del Monagrillo (Province de Murcie): âge radiométrique et corrélations avec les sédiments néogènes du basin de Hellin (Espagne). Académie des Sciences, Paris, Comptes Rendus, série D, 292, II, 1035–1038.

Berger, E. T. (1981) Enclaves ultramafiques, mégacristaux et leurs basaltes-hôtes en contexte océanique (Pacifique Sud) et continental (Massif Central Français). Thèse de Docteur ès Sciences Naturelles, Université Paris-Sud-Centre Orsay, 2 volumes, 469 p et 92 p.

Best, M. G., Henage, L. F., and Adams, J. A. S. (1968) Mica-peridotite, wyomingite and associated potassic igneous rocks in northeastern Utah. American Mineralogist, 53, 1041–1048.

Borley, G. D. (1967) Potash-rich volcanic rocks from southern Spain. Mineralogical Magazine, 37, 364–369.

Borsi, S., Ferrara, G., and Tongiorgi, E. (1967) Determinazione con il metodo del K/Ar delle eta delle rocce magmatiche delle Toscana. Bolletino delle Societa Geologica Italiana, 86, 403–410.

Boyd, F. R. and Nixon, P. H. (1978) Ultramafic nodules from the Kimberley pipes, South Africa. Geochimica et Cosmochimica Acta, 42, 1367–1382.

Brearley, M. and Scarfe, C. M. (1984) Dissolution of upper mantle minerals in alkali-basalt melt at 30 k bar: implications for ultramafic xenolith survival. (abstr.) Geological Society of America Abstracts with Programs, 16, 6.

Brooks, C. K., Noe-Nygaard, A., Rex, D. C., and Ronsbo, J. C. (1978) An occurrence of ultrapotassic dikes in the neighbourhood of Holsteinborg, West Greenland. Bulletin of the Geological Society of Denmark, 27, 1–8.

Bryan, W. B. (1970) Alkaline and peralkaline rocks of Socorro Island, Mexico. Carnegie Institution of Washington Year Book, 68, 194–200.

Cameron, K. L. and Cameron, M. (1973) Mineralogy of ultramafic nodules from Knippa quarry, Uvalde, Texas. Geological Society of America Abstracts with Programs, 5, 566.

Carmichael, I. S. E. (1967) The mineralogy and petrology of the volcanic rocks from the Leucite Hills, Wyoming. Contributions to Mineralogy and Petrology, 15, 24–66.

Charles, R. W. (1975) The phase equilibria of richterite and ferrorichterite. American Mineralogist, 60, 367–374.

Charles, R. W. (1977) The phase equilibria of intermediate compositions on the pseudobinary $Na_2CaMg_5Si_8O_{22}(OH)_2$–$Na_2Fe_5Si_8O_{22}(OH)_2$. American Journal of Science, 277, 594–625.

Civetta, L., Orsi, G., and Scandone, P. (1978) Eastwards migration of the tuscan anatectic magmatism due to anticlockwise rotation of the appennines. Nature, 276, 604–606.

Crittenden, M. D. and Kistler, R. W. (1966) Isotopic dating of intrusive rocks in the Cottonwood area, Utah. Geological Society of America Special Paper, 101, 298–299.

Cross, W. (1897) Igneous rocks of the Leucite Hills and Pilot Butte, Wyoming. American Journal of Science, 4, 115–141.

Danchin, R. V. and Boyd, F. R. (1976) Ultramafic nodules from the Premier kimberlite pipe, South Africa. Carnegie Institution of Washington Year Book 75, 531–538.

Dawson, J. B. (1980) Kimberlites and Their Xenoliths. Minerals and Rocks. Springer-Verlag, Heidelberg.

Dawson, J. B. and Smith, J. V. (1977) The MARID (mica–amphibole–rutile–ilmenite–diopside) suite of xenoliths in kimberlite. Geochimica et Cosmochimica Acta, 41, 309–323.

Delaney, J. S., Smith, J. V., Carswell, D. A., and Dawson, J. B. (1980) Chemistry of micas from kimberlites and xenoliths—II. Primary- and secondary-textured micas from peridotites xenoliths. Geochimica et Cosmochimica Acta, 44, 857–872.

Dickinson, J. E. and Hess, P. C. (1984) Rutile solubility and titanium coordination in silicate melts. In M. Brearley, Ed., Experimental Petrology Laboratory Annual Report. Department of Geology, The University of Alberta, Canada.

Edgar, A. D. and Arima, M. (1983) Conditions of phlogopite crystallization in ultrapotassic volcanic rocks. Mineralogical Magazine, 47, 11–19.

Edgar, A. D., Green, D. H., and Hibberson, W. C. (1976) Experimental petrology of a highly potassic magma. Journal of Petrology, 17, 339–356.

Eissen, J. P. (1982) Pétrologie comparée de basaltes de différents segments de zone d'accrétion océaniques à taux d'accrétion variés (Mer Rouge, Atlantique, Pacifique). Thèse 3ème cycle, Laboratoire de Minéralogie et Pétrographie, Strasbourg.

El Goresy, A. and Bernhardt, H. J. (1974) Taurus-Littraw TiO_2-rich basalts: opaque mineralogy and geochemistry. Proceedings of the Lunar Science Conference, 5, 627.

El Goresy, A. and Chao, E. C. T. (1976) Identification and significance of armalcolite in the Ries glass. Earth Planetary Science Letters, 30, 200.

Feraud, J., Fornari, M., Geffroy, J., and Lenck, P. (1977) Minéralisations arséniées et ophiolites: le filon à réalgar et stibine de Matra et sa place dans le district à Sb–As–Hg de la Corse alpine. Bulletin du BRGM (2), II, 2, 91–112.

Forbes, W. C. and Flower, M. F. J. (1974) Phase relations of titan-phlogopite $K_2Mg_4TiAl_2Si_6O_{20}(OH)_2$: a refractory phase in the upper mantle? Earth and Planetary Science Letters, 17, 339–356.

Fujimaki, H., Matsu-Ura, M., Aoki, K., and Sunagawa, I. (1981)

Ferropseudobrookite–silica material–albite–chondrule in the LH-77015 chondrite (L3). Memoirs of National Institute of Polar Research Special Issue, 20. Proceedings of the Sixth Symposium on Antarctic Meteorites.

Fuster, J. M. and Gastesi, P. (1965) Estudio petrologico de las rocas lamproiticas de Barqueros (Provincia de Murcia). Estudios Geologicos, 20, 299–314.

Fuster, J. M., Gastesi, P., Sagredo, J., and Fermoso, M. L. (1967) Las rocas lamproiticas del S.E. de Espana. Estudios Geologicos, 23, 35–49.

Ghiorso, M. S. and Carmichael, I. S. E. (1981) A Fortran IV computer program for evaluating temperatures and oxygen fugacities from the composition of coexisting iron–titanium oxides. Computers and Geosciences, 7, 123–129.

Gilbert, M. C., Helz, R. T., Popp, R. K., and Spear, F. S. (1982) Experimental studies of amphibole stability. In D. R. Veblen and P. H. Ribbe, Eds., Reviews in Mineralogy, Vol. 9B, chapter 2, p. 229–353. Mineralogical Society of America.

Haggerty, S. E. (1973) Armalcolite and genetically associated minerals in the lunar samples. Proceedings of the Lunar Science Conference, 4, 777.

Haggerty, S. E. (1975) The chemistry and genesis of opaque minerals. Physics and Chemistry of the Earth, 9, 295–307.

Haggerty, S. E. (1976) Oxidation of opaque mineral oxides in basalts. In Douglas Rumble, III, Ed., Oxide Minerals, Mineralogical Society of America, Short Course Notes, 3, Hg-1–Hg-100.

Helz, R. T. (1979) Alkali exchange between hornblende and melt: a temperature sensitive reaction. American Mineralogist, 64, 953–965.

Hentschel, G., Abraham, K., and Schreyer, W. (1980) First terrestrial occurrence of roedderite in volcanic ejecta of the Eifel, Germany. Contributions to Mineralogy and Petrology, 73, 127–130.

Hernandez-Pacheco, F. (1935) Estudio fisiographico y geologico del territorio comprendido entre Hellin y Cieza. Anales de la Universidad de Madrid (Ciencias), 4, 1–38.

Higuchi, H. and Nagasawa, H. (1969) Partition of trace elements between rock-forming minerals and the host volcanic rocks. Earth and Planetary Science Letters, 7, 281–287.

Jaques, A. L., Gregory, G. P., Lewis, J. D., and Ferguson, J. F. (1982) The ultrapotassic rocks of the West Kimberley region, Western Australia, and a new class of diamondiferous kimberlite. Third International Kimberlite Conference, Terra Cognita, 2, 251–252.

Jaques, A. L., Lewis, J. D., Smith, C. B., Gregory, G. P., Ferguson, J. F., Chappell, B. W., and McCulloch, M. T. (1984) The diamond-bearing ultrapotassic (lamproitic) rocks of the West Kimberley region, Western Australia. In J. Kornprobst, Ed., Kimberlites, I: Kimberlites and Related Rocks, p. 225–254. Elsevier, Amsterdam.

Jeremine, E. and Fallot, P. (1929) Sur la présence d'une variété de jumillite aux environs de Calasparra (Murcie). Académie des Sciences, Paris, Comptes Rendus, Série D, 188, 800.

Jones, A. P., Smith, J. V., and Dawson, J. B. (1982) Mantle metasomatism in 14 veined peridotites from Bultfontein Mine, South Africa. Journal of Geology, 90, 435–453.

Jones, A. P. and Smith, J. V. (1983) Petrological significance of mineral chemistry in the Agathla Peak and the Thumb minettes, Navajo volcanic field. Journal of Geology, 91, 643–656.

Kaplan, G., Faure, D., Elloy, R., and Heillamer, R. (1967) Contribution à l'étude de l'origine des lamproïtes. Bulletin du Centre de Recherches Exploration-Production Elf-Aquitaine, 1, 153–159.

Kohn, J. A. and Comeforo, J. E. (1955) Synthetic asbestos investigations, II: X-ray and other data on synthetic fluor-richterite, edenite and boron-edenite. American Mineralogist, 40, 410.

Kohn, J. A. and Hatch, R. A. (1955) Synthetic mica investigations, VI: X-ray and optical data on synthetic fluorphlogopite. American Mineralogist, 40, 10.

Kushiro, I. and Erlank, A. J. (1970) Stability of potassic richterite. Carnegie Institution Washington Year Book 68, 231–233.

Kuehner, S. M., Edgar, A. D., and Arima, M. (1981) Petrogenesis of the ultrapotassic rocks from the Leucite Hills, Wyoming. American Mineralogist, 66, 663–677.

Leake, B. E. (1978) Nomenclature of amphiboles. American Mineralogist, 63, 1023–1052.

Lewis, W. J. (1882) Krystallographische Notizen. Zeitschrift für Kristallographie, 7, 181–182.

Lloyd, F. E. (1981) Upper mantle metasomatism beneath a continental rift: clinopyroxenes in alkali mafic lavas and nodules from South West Uganda. Mineralogical Magazine, 44, 315–323.

McMahon, B. and Haggerty, S. E. (1984) The Bentfontein kimberlite sills: magmatic reactions and high intrusion temperatures. American Journal of Science, 284, 893–941.

Marvin, R. F., Hearn, B. C., Jr., Mehnert, H. H., Naeser, C. W., Zartman, R. E., and Lindsey, D. A. (1980) Late Cretaceous-Paleocene-Eocene igneous activity in North-Central Montana. Isochron/West, 29, 5–25.

Matson, R. E. (1960) Petrography and petrology of Smoky Butte intrusives, Garfield County, Montana. M. Sc. Thesis, Montana State University, Missoula.

Meyer, H. O. A. and McCallum, M. E. (1984) Mineral inclusions in diamonds from kimberlites in Colorado and Wyoming. (abstr.) Geological Society of America Abstracts with Programs, 16, 6.

Mitchell, R. H. (1981) Titaniferous phlogopite from the leucite lamproites of the West Kimberley area, Western Australia. Contributions to Mineralogy and Petrology, 76, 243–251.

Mitchell, R. H. and Hawkesworth, C. J. (1984) Geochemistry of potassic lavas from Smoky Butte, Montana. (abstr.) Geological Society of America Abstracts with Programs, 16, 6.

Montenat, C., Thaler, L., and Van Couvering, J. A. (1975) La faune de Rongeurs de Librilla. Corrélations avec les formations marines du Miocène terminal et les datations radiométriques du volcanisme de Barqueros (Province de Murcia). Académie des Sciences, Paris, Comptes Rendus, 281, 519–522.

Naeser, C. W. (1971) Geochronology of the Navajo-Hopi diatremes. Journal of Geophysical Research, 76, 4978–4985.

Nicholls, J. W. (1969) Studies of the volcanic petrology of the Navajo-Hopi, Arizona. Ph.D. Thesis, Geology, University of California, Berkeley.

Nicholls, J. W. and Carmichael, I. S. E. (1969) Peralkaline acide liquids: a petrological study. Contributions to Mineralogy and Petrology, 20, 268–294.

Niggli, P. (1923) Gesteins und Mineralprovinzen. Band I: Einführung. Verlag von Gebrüder Bornträger, Berlin.

Nixon, P. H. and Boyd, F. R. (1973) Petrogenesis of the granular and sheared ultrabasic nodule suite in kimberlite. In P. H. Nixon, Ed., Lesotho Kimberlites, p. 48–56. Lesotho National Development Corporation, Maseru, Lesotho.

Nixon, P. H., Thirwall, M. F., and Buckley, F. (1982) Kimberlite–lamproite consanguinity. Third International Kimberlite Conference, Terra Cognita, 2, 252–254.

Nobel, F. A., Andriessen, P. A., Hebeda, E. H., Priem, H. N. A., and Rondeel, H. E. (1981) Isotopic dating of the post-alpine Neogen volcanism in the betic Cordillera, Southern Spain. Geologie Minjbown, 60, 209–214.

Norrish, K. (1951) Priderite, a new mineral from the leucite-lamproites of the west Kimberley area, Western Australia. Mineralogical Magazine, 29, 496–501.

Olsen, E., Huebner, J. S., Douglas, J. A., and Plant, A. G. (1973) Meteoritic amphiboles. American Mineralogist, 58, 869–872.

Osann, A. (1906) Uber einige Alkaligesteine aus Spanien. Festschrift Rosenbusch, Stuttgart, 263–310.

Papike, J. T., Cameron, K. L., and Baldwin, K. (1974) Amphiboles and pyroxenes: characterization of other than quadrilateral components and estimates of ferric iron from microprobe data. Geological Society of America Abstracts with Programs, 6, 1053–1054.

Peck, L. C. (1964) Systematic analyses of silicates. U.S. Geological Survey Bulletin, 1170.

Peterson, E. U., Essene, E. J., Peacor, D. R., and Valley, J. W. (1982) Fluorine end member micas and amphiboles. American Mineralogist, 67, 538–544.

Post, J. E., Von Dreele, R. B., and Buseck, P. R. (1982) Symmetry and cation displacements in hollandites: structure refinements of hollandite, cryptomelane and priderite. Acta Crystallographica, B 38 (4), 1056–1065.

Prider, R. T. (1982) A glassy lamproite from the West Kimberley area, Western Australia. Mineralogical Magazine, 45, 279–282.

Raber, E. and Haggerty, S. E. (1979) Zircon oxide reactions in diamond bearing kimberlites. In F. R. Boyd and H. D. A. Meyer, Eds., Kimberlites, Diatremes and Diamonds: Their Geology, Petrology and Geochemistry, p. 299–240. American Geophysical Union, Washington, D.C.

Reid, A. M., Donaldson, C. H., Brown, R. W., Ridley, W. I., and Dawson, J. B. (1975) Mineral chemistry of peridotite xenoliths for the Lashaine volcano, Tanzania. Physics and Chemistry of the Earth, 9, 525–543.

Rice, J. M., Dickey, J. S., and Lyons, J. B. (1971) Skeletal crystallization of pseudobrookite. American Mineralogist, 56, 158–162.

Robert, J. L. (1976) Titanium solubility in synthetic phlogopite solid solution. Chemical Geology, 17, 213–227.

Robert, J. L. (1981) Etudes cristallochimiques sur les micas et les amphiboles. Applications à la pétrographie et à la géochimie. Thèse de Doctorat d'Etat, Université de Paris-Sud, Orsay.

Robert, J. L. and Chapuis, G. (1982) Crystal chemistry of Ti-rich micas: presence of MgIV and petrological consequences. 13th General Meeting, International Mineralogical Association 82, Varna, Bulgaria.

Rock, N. M. S. (1984) Nature and origin of calc-alkaline lamprophyres: minettes, vogesites, kersantites and spessartites. Transactions of the Royal Society of Edinburgh: Earth Sciences, 74, 193–227.

Roden, M. F. (1981) Origin of coexisting minette and ultramafic breccia, Navajo volcanic field. Contributions to Mineralogy and Petrology, 77, 195–206.

Ruiz, J. L. and Badiola, E. R. (1980) La region volcanica neogena del sureste de Espana. Estudios Geologicos, 36, 5–63.

Sack, R. (1982) Spinels as petrogenetic indicators: activity-composition relations at low pressure. Contributions to Mineralogy and Petrology, 79, 169–186.

San Miguel de la Camara, M., Almela, A., and Fuster, J. M. (1952) Sobre un volcan de veritas recientemente descubierto en el Mioceno de Barqueros (Murcia). Estudios Geologicos, 7, 411–429.

Scarfe, C. M., Takahashie, E., and Yoder, H. S. (1980) Rates of dissolution of upper mantle minerals in an alkali-olivine basalt melt at high pressures. Carnegie Institution of Washington Year Book 79, 290–296.

Scott, B. H. (1981) Kimberlite and lamproite dikes from Holsteinborg, West Greenland. Geoscience Journal, 4, 3–23.

Scott Smith, B. H. and Skinner, E. M. W. (1984) Diamondiferous lamproites. Journal of Geology, 92, 433–438.

Seifert, F. and Schreyer, W. (1971) Synthesis and stability of micas in the system K_2O–MgO–SiO_2–H_2O and their relations to phlogopite. Contributions to Mineralogy and Petrology, 30, 196–215.

Sheraton, J. W. and England, R. N. (1980) Highly potassic mafic dikes from Antarctica. Journal of the Geological Society of Australia, 27, 129–135.

Simkin, T. and Smith, J. V. (1970) Minor-element distribution in olivine. Journal of Geology, 78, 304–325.

Smith, J. V. (1974) Feldspar Minerals (2). Springer-Verlag, Berlin.

Stefanini, G. (1934) Il complesso eruttivo di Orciatico e Montecatini in provincia di Pisa. Atti Societa Toscana Scienze Naturali, Memorie, 44, 224–300.

Tateyama, H., Shimoda, S., and Sudo, T. (1974) The crystal structure of the synthetic MgIV mica. Zeitschrift für Kristallographie, 139, 196–206.

Valley, J. W., Peterson, E. U., Essene, E. J., and Bowman, J. R. (1982) Fluorphlogopite and fluortremolite in Adirondack marbles and calculated C, O, H, F fluid compositions. American Mineralogist, 67, 545–557.

Van Kooten, G. K. (1980) Mineralogy, petrology and geochemistry of an ultrapotassic basaltic suite, Central Sierra Nevada, California, U.S.A. Journal of Petrology, 21, 651–684.

Velde, D. (1967) Sur un lamprophyre hyperalcalin potassique: la minette de Sisco (Corse). Bulletin de la Société Française de Minéralogie et de Cristallographie, XC, 214–223.

Velde, D. (1968) A new occurrence of priderite. Mineralogical Magazine, 36, 867–870.

Velde, D. (1969) Minettes et kersantites. Une contribution à l'étude des lamprophyres. Thèse de Doctorat d'Etat, Faculté des Sciences, Paris.

Velde, D. (1975) Armalcolite–Ti-phlogopite–diopside–analcite bearing lamproites from Smoky Butte, Garfield County, Montana. American Mineralogist, 60, 566–573.

Velde, D. (1978) An aenigmatite–richterite–olivine trachyte from Puu Koae, West Maui, Hawaii. American Mineralogist, 63, 771–778.

Velde, D. (1979) Trioctahedral mica in melilite-bearing eruptive rocks. Carnegie Institution of Washington Year Book, 78, 468–475.

Velde, D. and Yoder, H. S. (1983) Partitioning of iron and magnesium between melilite, olivine, and clinopyroxene in lavas. Carnegie Institution of Washington Year Book, 82, 256–264.

Von Knorring, O. V. and Cox, K. G. (1961) Kennedyite, a new mineral of the pseudobrookite series. Mineralogical Magazine, 32, 676–682.

Wade, A. and Prider, R. T. (1939) The leucite-bearing rocks of the West Kimberley area, Western Australia. Quarterly Journal of the Geological Society (London), 96, 39–98.

Watson, E. B. (1979) Calcium content of forsterite coexisting with silicate liquid in the system Na_2O–CaO–MgO–Al_2O_3–SiO_2. American Mineralogist, 64, 824–829.

Wendlandt, R. F. and Eggler, D. H. (1980) The origin of potassic magmas: 1—Melting relations in the systems $KAlSiO_4$–Mg_2SiO_4–SiO_2 and $KAlSiO_4$–MgO–SiO_2–CO_2 to 30 kbar. American Journal of Science, 280, 385–420.

Williams, H. (1936) Pliocene volcanoes of the Navajo-Hopi country. Bulletin of the Geological Society of America, 47, 111–172.

Wörner, G., Beusen, J.-M., Duchateau, N., Gijbels, R., and Schmincke, H.-U. (1983) Trace element abundances and mineral/melt distribution coefficients in phonolites from the Laacher See volcano (Germany). Contributions to Mineralogy and Petrology, 84, 152–173.

Manuscript received, March 27, 1984;
accepted for publication, September 3, 1985.